

2023

# Investigations of enterotoxigenic E. Coli (ETEC) intestinal colonization in neonatal mice and human shedding of panchol, a new live attenuated oral cholera vaccine

---

<https://hdl.handle.net/2144/48403>

*Downloaded from DSpace Repository, DSpace Institution's institutional repository*

BOSTON UNIVERSITY

ARAM V. CHOBANIAN & EDWARD AVEDISIAN SCHOOL OF MEDICINE

Thesis

**INVESTIGATIONS OF ENTEROTOXIGENIC *E. COLI* (ETEC) INTESTINAL  
COLONIZATION IN NEONATAL MICE AND HUMAN SHEDDING OF  
PANCHOL, A NEW LIVE ATTENUATED ORAL CHOLERA VACCINE**

by

**BRYAN WANG**

B.S., Emory University, 2021

Submitted in partial fulfillment of the  
requirements for the degree of  
Master of Science

2023

© 2023 by  
BRYAN WANG  
All rights reserved

Approved by

First Reader

---

Lee Wetzler, M.D.  
Professor of Medicine and Microbiology

Second Reader

---

Matthew K. Waldor, M.D., Ph.D.  
Edward H. Kass Professor of Medicine  
Brigham and Women's Hospital  
Harvard University, School of Medicine

## **DEDICATION**

I would like to dedicate this work to my family for their never-ending support.

## **ACKNOWLEDGMENTS**

I would like to thank all my advisors and professors at the BU Aram V. Chobanian and Edward Avedesian School of Medicine as well as Dr. Matthew K. Waldor, M.D., Ph.D. and Dr. Deborah Leitner, Ph.D., as both mentors and teachers.

**INVESTIGATIONS OF ENTEROTOXIGENIC *E. COLI* (ETEC) INTESTINAL  
COLONIZATION IN NEONATAL MICE AND HUMAN SHEDDING OF  
PANCHOL, A NEW LIVE ATTENUATED ORAL CHOLERA VACCINE**

BRYAN WANG

ABSTRACT

**Background:** *Vibrio cholerae* and Enterotoxigenic *E. Coli* (ETEC) are enteropathogens that are global causes of cholera and traveler's diarrhea which are responsible for millions of diarrhea cases every year. ETEC and cholera are primarily found in Sub-Saharan Africa and Asia, particularly in nations with inadequate sanitation systems or little access to clean water. Infants and children are most vulnerable to these diseases, as severe infections can lead to stunting and death. The incidence of cholera and ETEC diarrhea have increased, due in part to changing weather patterns. At present, robust animal models for studies of ETEC colonization are lacking to study colonization and bottlenecks. The only licensed vaccines against cholera in endemic countries are killed whole cells, however, new live attenuated oral cholera vaccines (OCV) are in development and offer significant advantages. PanChol is a live attenuated OCV entering phase I trials.

**Specific Aims:** To propel studies of ETEC pathogenesis, I attempted to create a suckling mouse model of this globally important pathogen. To accomplish this goal, I constructed barcoded ETEC libraries that enabled me to determine founding population sizes along with intestinal ETEC burdens. To better understand PanChol, a new live attenuated OCV,

I studied the shedding of the vaccine in the first 3 human volunteers to ingest this novel agent.

**Methods:** Triparental mating of donor strains MFD $\lambda$ pir pJMP1039 and MFD $\lambda$ pir pSM1 with recipient ETEC strains enabled construction of barcoded libraries. Neonatal CD-1 and C57BL/6 mice were infected with  $10^4$ - $10^7$  CFU of wild type ETEC to develop an infant mouse model. Founding population sizes of ETEC strains were compared via sequencing and STAMPR analysis while CFU burdens were determined via plating. Shedding of PanChol was done through enumeration of serial dilutions of fecal samples. Serotyping of shed PanChol was carried out using anti-Ogawa and anti-Inaba antisera.

**Results:** There were marked differences in ETEC small intestinal colonization in different mouse strains. Outbred CD-1 suckling mice only colonized with a  $10^7$  dose. In contrast, colonization of ETEC was approximately  $10^6$  CFU per small intestine at inoculum sizes of  $10^5$  or greater in C57BL/6 mice. Laboratory studies using simulated bottlenecks made by serial dilutions established that the barcoded libraries accurately reflect founding population sizes up to  $10^5$  CFU. There was no difference in founding population sizes at the same inoculum size between WT ETEC and a hypervesiculation  $\Delta mlaE$  mutant, though the founding population size increased with increasing input. PanChol retained the Hikojima serotype and shedding occurred in all volunteers with maximum colonization occurring 3 days post administration of  $10^6$  CFU.

**Conclusions:** C57BL/6 P5 mice can serve as a new model to study ETEC intestinal colonization. Hypervesiculating ETEC did not produce a difference in founding



population or colonization at the same input as WT ETEC strains. PanChol shows great promise as a viable OCV with shedding at  $10^6$  input and no serotype reversion.

## TABLE OF CONTENTS

DEDICATION.....	iv
ACKNOWLEDGMENTS .....	v
ABSTRACT.....	vi
TABLE OF CONTENTS.....	ix
LIST OF FIGURES .....	xii
LIST OF ABBREVIATIONS.....	xiii
INTRODUCTION .....	1
Cholera and Traveler’s Diarrhea Epidemiology.....	2
Climate Change and Diarrheal Pathogen Outbreaks .....	3
Vulnerable Populations to Enteropathogens.....	4
ETEC and <i>V. cholerae</i> Ecology.....	6
ETEC and <i>V. cholerae</i> Classification .....	7
ETEC and <i>V. cholerae</i> Mechanisms of Virulence.....	8
Immune Response to ETEC and <i>V. cholerae</i> .....	9
Disease Symptoms and Current Treatments.....	11
<i>V. cholerae</i> Vaccines .....	12
The Case for Live Attenuated OCVs for ETEC and <i>V. cholerae</i> .....	14
Outer Membrane Vesicles and the Mla Pathway.....	16
OMV Vaccine Implications .....	19
SPECIFIC AIMS .....	20
METHODS .....	22

Barcoding of ETEC .....	22
Pooled ETEC Library Formation.....	23
Sequencing and STAMPR.....	24
OMV Isolation .....	24
OMV Protein Concentration.....	25
Neonatal Mouse ETEC Infection Model .....	25
Dose Specific ETEC Colonization .....	26
Growth Curve of ETEC Strains .....	26
Thiosulfate-Citrate-Bile Salts-Sucrose Agar (TCBS) Plates .....	27
Quantitative and Qualitative Analysis of PanChol.....	27
Serotyping of PanChol.....	28
Statistical Analysis.....	28
Animal Use Statement .....	28
RESULTS .....	29
DISCUSSION.....	38
OMV Amounts in Wild type and Mutant ETEC .....	38
Barcoding and STAMPR Analysis of ETEC Strains.....	39
Neonatal Mouse Model of Infection with ETEC.....	39
Founding Population and Colonization of Barcoded ETEC Strains.....	41
PanChol Shedding and Stability .....	42
Limitations .....	43
Future Directions and Implications for Further Research .....	44

BIBLIOGRAPHY.....	46
CURRICULUM VITAE.....	56

## LIST OF FIGURES

Figure 1. OMV biogenesis via Mla pathway .....	17
Figure 2. Protein concentration from OMV isolates.....	29
Figure 3: Barcode frequency distribution of ETEC libraries.....	30
Figure 4. Raw barcode reads of ETEC pooled libraries. ....	31
Figure 5. In vitro STAMPR standard curves of barcoded ETEC strains.....	31
Figure 6. Growth curve of barcoded and non-barcoded ETEC Strains. ....	32
Figure 7. ETEC WT colonization in P5 neonatal mice .....	33
Figure 8. Colonization and founding population of barcoded WT and $\Delta mlaE$ ETEC .....	34
Figure 9. Stool shedding of PanChol in human subjects. ....	36

## LIST OF ABBREVIATIONS

BC	Barcode
Carb	100 mg/mL Carbomycin
CF	Colonization Factors
CFTR	Cystic Fibrosis Transmembrane Regulator
CFU	Colony Forming Units
Ctx	Cholera Toxin
Ctx-A	Cholera Toxin A Subunit
Ctx-B	Cholera Toxin B Subunit
CU	Chaperone-Usher Pili
DAP	Diaminopimelic Acid
ETEC	Enterotoxigenic <i>E. Coli</i>
FA	Fatty Acids
Kan50	50 mg/mL kanamycin
KDO	3-deoxy-d-manno-2-octulosonic acid
LMIC	Low and Middle Income Countries
LPO	Lipopolysaccharide
LT	Heat Labile Toxin
OCV	Oral Cholera Vaccine
OMV	Outer Membrane Vesicle
OSP	O-Specific Polysaccharide Antigen
PCR	Polymerase Chain Reaction

PES.....	Polyethersulfane
SI.....	Small Intestine
Sm200.....	200 mg/mL Streptomycin
ST.....	Heat Stable Enterotoxin
STAMPR .....	Sequence Tag-based Analysis of Microbial Population Dynamics
T4P .....	Type IV Pili
TCBS .....	Thiosulfate–Citrate–Bile Salts–Sucrose Agar
TCP .....	Toxin Coregulated Pilus
UN.....	United Nations
UNICEF .....	United Nations Children Fund
WT .....	Wild type

## INTRODUCTION

The development of next generation live attenuated vaccines has great potential to combat global enteropathogens such as *Vibrio cholerae* and Enterotoxigenic *E. coli* (ETEC). ETEC shares many similarities with *V. cholerae*; they overlap in geographical distribution, modes of pathogenesis, virulence factors, and can both colonize the intestinal tract. *V. cholerae* causes the disease cholera that is characterized by vomiting, dehydration and the hallmark symptom of severe watery diarrhea, often referred to as rice water stool. ETEC is the most common cause of traveler's diarrhea, also known as "Montezuma's revenge" which is similar to cholera, but usually less severe. Cholera and traveler's diarrhea are caused by ingestion of contaminated food or water. Due to the fecal-oral transmission of both ETEC and *V. cholerae*, the disease is most prevalent in low and middle income countries (LMIC) that lack adequate sanitation systems and access to clean water. Both *V. cholerae* and ETEC can lead to severe diarrhea and mortality when left untreated, predominantly affecting children and infants, who are the most vulnerable. As climate change causes greater extremes in weather, cholera and ETEC associated diarrhea have been on the rise. There is currently no commercially available vaccine for ETEC, however, there are ETEC vaccines undergoing clinical trial. The only WHO approved cholera vaccines are killed whole cell vaccines that require two doses and have reduced efficacy in children less than 5 years of age. The development of next generation live attenuated cholera and ETEC vaccines offers great promise to address the resurgence of cholera and to reach the WHO goal of ending cholera by 2030.



### ***Cholera and Traveler's Diarrhea Epidemiology***

Cholera is a global disease but is most prevalent in Sub-Saharan Africa and parts of Asia. There are approximately 3 million cholera cases and 100,000 deaths every year (*Cholera*, n.d.). The 7th cholera pandemic began in 1961 and spread from its origin in Indonesia to Eurasia, South Asia, Europe, Africa and eventually reached the Americas in 1991. More than 30 nations, many of which are in the East Mediterranean and Africa, have reported cholera outbreaks, half of which did not have outbreaks prior to 2021. The average case fatality ratio in 2022 increased to 3% in Africa and 1.9% globally (*Cholera – Global Situation*, n.d.). A common theme in the current pandemic has been the link between increasing cholera cases and extreme weather patterns, political instability, urbanization, and population displacement. Haiti had its first outbreak in 2010 ten months after a 7.0 magnitude earthquake led to a humanitarian crisis. The dispatch of United Nations Stabilization Mission in Haiti Troops from Nepal led to a cholera outbreak due to improper sewage disposal into the local river system from the visiting humanitarian effort. Genomic analyses revealed that the pathogen originated from southeast Asia. Although the 2010 epidemic officially ended in January of 2019, cholera re-emerged in October 2022 in areas surrounding Port-au-Prince, the Haitian capital, and has spread to much of the nation. Political instability caused by violent gang takeovers in the wake of the President Jovenel Moïse's assassination in 2021 have led to a shortage in food, water, and fuel as well as a decay in government infrastructure, all of which have exacerbated the epidemic. As of January 2023, there have been more than 25,000 reported cases and 500 deaths in Haiti (Ocasio, 2023).

Like cholera, ETEC infections are a global phenomenon which occur in developed and developing nations alike. There are approximately 220,000,000 ETEC cases and more than 70,000 deaths annually (Khalil et al., 2018). ETEC transmission may occur across vast distances via contaminated food-products. There are an estimated 40,000 annual ETEC cases in the United States, which have largely been associated with travel and international foodborne transmission (Scallan et al., 2011). LMICs in Africa and East Mediterranean region have the highest burden of ETEC mortality and morbidity with about 44,000 deaths in children 5 years old or younger (Qadri et al., 2005). Though the death rate from ETEC infections has declined over the past couple decades, morbidity rates have not significantly decreased.

### ***Climate Change and Diarrheal Pathogen Outbreaks***

Though most outbreaks occur in drought/flood-free conditions, extreme weather patterns associated with climate change increase the risk of ETEC and cholera epidemics. Approximately 30% of droughts and 7% of floods in Sub-Saharan Africa led to cholera outbreaks (Rieckmann et al., 2018). Floods overwhelm sewage and sanitation systems and introduce wastewater into the environment, putting people in direct contact with contaminated water in nations where fresh water is not readily accessible. Droughts are also correlated with cholera epidemics as there is less access to water and thus a decrease in hygiene. The number of cholera cases during a drought is 4.5 times greater compared to seasonal flooding, likely due to the difference in duration between the two weather patterns (Rieckmann et al., 2018). Monsoon flooding of Bangladesh has historically led to spikes

in both ETEC and cholera cases as much of the nation is geographically characterized as a flood plain (Harris et al., 2008). A large contributing factor to increasing African cholera outbreaks in 2022 has been the cyclical dry and wet season which have been exacerbated due to climate change as La Nina climatic phenomenon and its subsequent monsoons and cyclones are exacerbated. In nations with little to no centralized system for water sanitation and delivery, people are forced to dig wells, take water from the watershed or reuse water for conservation during a drought, all of which can introduce sources of contamination and spread pathogenic bacteria between people. In Malawi, abnormal amounts of flooding because of tropical storm Ana and Cyclone Gombe, lack of access to safe water and ritual burials have led to 31,241 reported cases of cholera as of January 2023, the worst outbreak since the 2002 epidemic (*Cholera - Malawi*, n.d.).

### ***Vulnerable Populations to Enteropathogens***

Both *V. cholerae* and ETEC infection can occur in all ages and genders, however, the most vulnerable populations are children and infants. Every year, approximately 35,900 children under the age of 5 have died due to ETEC infection in LMICs, 50% of which occur in India, Nigeria, the Democratic Republic of Congo, and Pakistan (Anderson et al., 2019). The number of children who have died from ETEC symptoms and ETEC related stunting has increased to approximately 44,400 deaths, though the exact number of cases is unknown as clinical validation of infection is not always readily available in endemic areas (Anderson et al., 2019). Diagnosis and cataloging of cases is often done through qualitative methods such as presence of hallmark symptoms. Children and infants are more

prone to severe diarrhea due to their high intestine surface area to body weight ratio and do not have robust, mature immune systems. Cholera and ETEC infections related symptoms may not only exacerbate symptoms and existing health complications, but they can further lead to future health complications (Rodríguez et al., 2011). Stunting is a common consequence of early enteric infections that can lead to decreased physical growth and neurodevelopment as well as a higher risk of chronic diseases and repeat infections. Childhood malnutrition, wasting, dehydration have been associated with increases in mortality and morbidity from cholera and ETEC infection, all of which have a socioeconomic and cultural link. In countries where cholera and ETEC are most prevalent, food insecurity and reduced access to clean water can lead to a higher reliance on contaminated sources of water and food. Studies have shown that underweight children were more likely to have longer hospitalizations and increased duration of diarrhea (Nuzhat et al., 2022). The mortality rate of children with severe acute malnutrition is three times higher compared to those without (Roy et al., 2011). Undernutrition can lead to a decrease in gastric secretion and acidity of gastric fluid in the stomach. The structure and function of the intestinal mucosa is greatly affected. The thickness of the tissue layers of the small intestine wall is greatly reduced, resulting in the characteristic “tissue paper intestine” (Rodríguez et al., 2011). Abnormal villous and microvillous morphology in addition to increased intestinal permeability greatly contributes to bacterial proliferation/colonization of the gastrointestinal tract. Malnourished children have an increase in lymphocyte infiltration into the tissue layers of the small intestine, however, there is a decrease in immune responsiveness (Rytter et al., 2014). Notably, granulocytes were seen to have

markers for apoptosis and had greater DNA damage. Lymphatic tissues have been shown to be depleted of lymphocytes. Antimicrobial secretions, such as secretory IgA are lower in children compared to adults and are significantly lower in those with protein-calorie malnutrition (Rytter et al., 2014). The effects of malnutrition not only increase virulence and severity of symptoms, but the increased colonization leads to increased shedding through greater diarrhea volume and duration, presenting a significant risk to the surrounding community. Children and infants not only are predisposed for more severe infections, but malnourishment exacerbates symptoms and often leads to higher rates of mortality and longer-term health complications.

### ***ETEC and V. cholerae Ecology***

*V. cholerae* and ETEC are both aquatic Gram-negative bacteria. Vibrios naturally inhabit coastal aquatic environments, namely brackish and freshwater environments around the globe. Both pathogens readily bind to both abiotic and biotic surfaces, such as chitin, leading to biofilm formation using pili, membrane surface proteins, and other colonization factors (Lutz et al., 2013). Biofilms are critical for environmental adaptation and stress response and are composed of colonies of bacteria scaffolded in a matrix of nucleic acids, proteins, and polysaccharides. Under suboptimal conditions, *Vibrios* may persist in the environment in a viable but nonculturable state, but readily resuscitate in animal hosts. Attachment and colonization on various prokaryotic and eukaryotic aquatic organisms, such as shellfish and zooplankton, can spread to higher level consumers like tilapia and gulls (Laviad-Shitrit et al., 2019). Aquatic plants are a large reservoir for ETEC,

which also has ecological niches on the leaves and fruits. Both ETEC and *V. cholerae* are ingested by animals where the intestinal environment causes an upregulation of various virulence genes. *V. cholerae* and ETEC rapidly colonize and proliferate in the intestine of various aquatic and nonaquatic animals and are shed into the environment through fecal matter (Lutz et al., 2013).

### ***ETEC and V. cholerae Classification***

*V. cholerae* can be classified into different serogroups, serotypes, and biotypes. Serogroups of *V. cholerae* are categorized by the lipopolysaccharide (LPS) O-Antigen. The lipopolysaccharides (LPS) structure includes a lipid A insertion into the outer leaflet of the outer membrane, followed by 3-deoxy-d-manno-2-octulosonic acid (KDO), inner and outer polysaccharide cores and a variable O-antigen comprised of oligosaccharide subunits. The O1 serotype has been the primary driver of all pandemics, however the O139 serogroup led to an epidemic in southeast Asia in 1992. The O139 serogroup is no longer prevalent. Non O1 or O139 serogroups are known as non-agglutinating Vibrios (NAGs). NAGs are rarely the source of cholera outbreaks, though they have been observed before in the stool of those with diarrhea (Hasan et al., 2012). Serotypes are defined by methylation of the O1 O-antigen. The Ogawa serotype is 100% methylated, while the Hikojima serotype is 50% methylated and the Inaba variant is unmethylated. Similar to *V. cholerae*, ETEC can be classified into serogroups based on the O-antigen, but classification of strains can also include the H-antigen, colonization factors and toxins (Wolf, 1997). ETEC H10407 is a prototypical strain which is classified specifically as O78:H11:K80.

### ***ETEC and V. cholerae Mechanisms of Virulence***

Cholera is caused by *V. cholerae* penetration into the mucus layer of the small intestine, colonization of microvilli and deployment of cholera toxin (Ctx). This enterotoxin and the toxin co-regulated pilus (TCP) are both crucial for virulence and colonization. *V. cholerae* produces diarrheal symptoms due to the production of Ctx. The genes encoding Ctx are part of the genome of a filamentous bacteriophage, CTX $\Phi$ , that integrated into pandemic strain *V. cholerae* genomes (Waldor & Mekalanos, 1996). TCP, whose expression is co-regulated with Ctx, is necessary for the formation of microcolonies which help *V. cholerae* to evade immune cells, increase toxigenicity, and colonize the small intestine. TCP consists of pilin subunits which are structured into a homopolymer and is the receptor for CTX $\Phi$ . Ctx is classified as an AB<sub>5</sub> type toxin which consists of two subunits, A (Ctx-A) and B (Ctx-B). The A subunit of Ctx-A has 2 domains, A1 and A2, which are bound together through a disulfide bond. The A1 domain acts as the catalytic domain and the A2 domain anchors the A subunit to the B subunit, which binds to a cellular receptor that allows the import of the toxin holoenzyme (Beddoe et al., 2010). The B subunit is a homo-pentamer of which each monomer has a receptor binding site. The AB<sub>5</sub> class of toxin can be found in many virulent bacterial pathogens and share similar homologies, such as the oligosaccharide or oligonucleotide binding scaffolds. The structure of Ctx shares 80% homology with the heat labile enterotoxin (LT) found in ETEC (Mudrak & Kuehn, 2010). Both Ctx and LT lead to the activation of adenylate cyclase which activates protein kinase A through an increase in cyclic adenosine monophosphate

(Ramamurthy et al., 2020). Phosphorylation of cystitis fibrosis transmembrane regulator (CFTR) by activated PKA leads to increased water movement into the intestinal lumen and diarrhea. In addition to LT, ETEC utilizes heat stable enterotoxin (ST), which also leads to the activation of CFTR, but uses the guanylate cyclase C signal transduction pathway via extracellular cellular binding. More than 25 colonization factors (CF) in ETEC have been implicated in pathogenesis and proliferation in humans. Colonization factors in ETEC are typically pili, or fimbriae, which are found on the outer membrane surface and are non-flagellar filamentous polymeric protein structures. ETEC colonization factors can be divided largely into two groups based on their assembly pathways: chaperone-usher pili (CU) and type IV pili (T4P). CU colonization factors comprise the majority of colonization factors with CFA/I and CS1-6 typically found in ETEC isolates from diarrheal volunteers (Vidal et al., 2019). Structurally, CUs are made up of a major and minor subunit and rely on an usher and chaperone protein for assembly. The two T4P colonization factors are CS21 “longus” and CS8 (CFA/III) which are used for binding to various surfaces, signal transduction, formation of biofilm and various other biological functions which all contribute to ETEC pathogenesis (Craig et al., 2004). Approximately 20% of ETEC colonization factors are currently unknown (Isidean et al., 2011).

### ***Immune Response to ETEC and V. cholerae***

Innate immune defenses against *V. cholerae* and ETEC include the intestine mucus layer, antimicrobial proteins, and toll-like receptor-mediated signaling pathways (Ramamurthy et al., 2020). *V. cholerae* is more sensitive to low pH than ETEC and



challenge studies have shown that high colonization is capable with low CFU input when gastric acid is alkalinized (Nhu et al., 2021). In general, the innate immune defense for ETEC and *V. cholerae* is similar. The mucus layer of the small intestine (SI) is a critical component of pathogen defense as it contains various antimicrobial proteins, sIgA, IgG and IgM and physically prevents colonization of the enteroepithelial surface (Ramamurthy et al., 2020). Both ETEC and *V. cholerae* stimulate increased production of interleukin-8 (Long et al., 2016). Though not directly apart of the innate immune system, microbiota can also influence immune response and colonization of enteropathogens through the promotion of mucosal barrier function by stimulating production of mucus, immune response, and antimicrobial compounds from epithelial cells (Belkaid & Hand, 2014). The microbiota can also directly compete with pathogenic bacteria and prevent colonization through production of secondary bile salts, short chain fatty acids and inhibitory substances (Rolhion & Chassaing, 2016). Innate immune responses act as the first line of defense and lead to activation of the adaptive immune system. Primary adaptive immune defense against cholera utilizes vibriocidal antibodies against the O antigen polysaccharides displayed to Peyer's patches in the GI mucosa (Bhuiyan et al., 2009). Ctx-B causes activation of the adaptive immune system through both inflammasomes and interleukin production via macrophages, which eventually lead to the production of Ctx-B IgG and IgA antibodies. Cholera toxin also leads to increased differentiation of CD4<sup>+</sup> T cells as well as cytotoxic CD8<sup>+</sup> T cells. O-specific polysaccharide antigen (OSP) immune responses offer greater protection compared to Ctx-B (Hossain et al., 2019). Immune responses to Ctx are not long term as Ctx-IgG and levels of Ctx-IgA decrease over time (Ramamurthy

et al., 2020). Antibodies bind to antigens and prevention of enteropathogen-enterocyte interaction leads to a reduction of diarrhea and intestinal colonization of both *V. cholerae* and ETEC. Adaptive immune response to ETEC is based on a combination of antigens which include LT, CFs (CFA/I, CS21, etc.) as well as other intracellular proteins such as EatA autotransporter and EtpA adhesin, all of which lead to increased serum IgA and IgG production (Chakraborty et al., 2016). Collectively, the immune system and human gut microbiota, along with other factors, influence the host bottleneck which greatly reduces the original bacterial inoculum to a small founding population which will entirely represent the genetic diversity of colonization (Abel et al., 2015). Analysis of the bottleneck and the resulting founding population can help uncover host-pathogen interactions.

### ***Disease Symptoms and Current Treatments***

Both cholera and traveler's diarrhea have very similar symptoms. The incubation period between *V. cholerae* and ETEC is comparable: between 10 hours to a couple days (Azman et al., 2013). Those who are asymptomatic or have mild symptoms can still shed bacteria via fecal matter (Nelson et al., 2009). Severe symptoms include vomiting, severe watery diarrhea, and nausea as well as rapid heart rate, low blood pressure, kidney failure and dehydration. Mortality is caused by dehydration due to loss of fluids through stool (Khalil et al., 2018). A hallmark symptom of cholera is rice water diarrhea which occurs during the early stages of infection and contains high concentrations of *V. cholerae* (Harris et al., 2012). Current treatments for cholera and ETEC are a combination of antibiotics and oral or intravenous rehydration. Current antibiotics for cholera include doxycycline,

ciprofloxacin, and azithromycin (Nelson et al., 2011). Traveler's diarrhea treatment typically includes hydration in combination with fluoroquinolone antibiotics only in severe cases as ETEC is resistant to many common antibiotics, including doxycycline (Sharma et al., 2017).

### ***V. cholerae Vaccines***

Current vaccines for cholera are oral cholera vaccines (OCV) which differ from the first cholera vaccine in 1885 which was an intramuscular injection of live isolated *V. cholerae*. Tested OCVs have been both live attenuated and killed. Dukoral is a killed/inactivated OCV that is a combination of O1 classical Ogawa, Inaba and El Tor Inaba (Sit et al., 2022). The strain composition of Dukoral was determined through epidemiological studies that suggested that severe infections can lead to decrease in repeat infections (Lopez et al., 2014). Further investigation into the significance of serotypes for protection suggested that only El Tor Inaba led to protection against both Inaba and Ogawa serotypes (Ali et al., 2011). Dukoral was first field tested in Bangladesh in 1985 and clinical trials indicated that the introduction of Ctx-B provided protective benefit, however the immunogenic benefit was short lived (Sit et al., 2022). It was also observed that efficacy of Dukoral may be dependent on blood type as the O blood group had less protection to El Tor Ogawa (Song et al., 2021). Derivatives of Dukoral were developed by adding killed O139 strains in response to the outbreaks in Asia in the 1990s, resulting in the formation of ShanChol, Euvichol and mORCvax (Sit et al., 2022). Of the vaccines commercially available, only ShanChol, Dukoral and Euvichol (Plus) are prequalified by the WHO and

are recommended to UNICEF and the UN for distribution. The regimen for killed OCVs is two doses, however, the time between doses varies. Doses for Dukoral are administered 1 week apart for those over the age of 6 and three doses are administered for those between 2 and 6 years of age. Shanchol and mORC-Vax have a 2-week interval between doses and are given for those at least one and two years of age, respectively. Hillchol is a new killed OCV engineered to be a Hikojima serotype and is currently in a phase III clinical trial. Increased deployment and usage of OCVs can impart herd immunity as seen in Africa and South Asia, increasing protection for those who have not been immunized. Using mathematical modeling based on data obtained from Bangladesh predicted that herd immunity could confer an 89% reduction in cholera cases among unvaccinated (Longini et al., 2007). Live attenuated OCVs are genetically altered *V. cholerae* which colonize the small intestine and stimulate an immune response from a myriad of antigens, but particularly the O-antigen. Development of live attenuated OCVs began with the advancement of genetic engineering allowing the deletion of genes encoding the cholera toxin and various other virulence factors (Sit et al., 2022). Early development of live OCVs were not viable, as clinical trials revealed high incidences of adverse symptoms, however, enhanced immunogenicity compared to killed vaccines prompted further interest. Specific genetic manipulations are used to remove toxins and import immunogenic antigens, such as Ctx-B. In 2016 Vaxchora was approved by the FDA and remains the sole live attenuated OCV available approved by the FDA. No live attenuated OCVs have been pre-certified by the WHO.

### ***The Case for Live Attenuated OCVs for ETEC and V. cholerae***

Though cholera vaccination has primarily utilized and relied on killed OCVs, there is a growing interest in and need for next generation, live attenuated OCVs. Heat or formalin inactivated OCVs have significant limitations. The need for repeated administrations as well as decreased effectiveness in children less than five years of age and against current cholera strains present serious challenges in the face of increasing natural disasters and cholera epidemics (Sit et al., 2022). Though killed OCVs retain immunogenic O-antigen of LPS, heat or formalin may denature proteins and decrease the range of immune responses (di Tommaso et al., 1994). Dukoral clinical trials in Bangladesh found diminished immune protection following three years of administration and no protection after 5 years (van Loon et al., 1996). Dukoral requires a booster dose every 2 years for those older than 6 years and every 6 months for those between 2 and 6 years old. There is also a week delay between administration of doses and protection. Shanchol requires a booster dose every two years (Saluja et al., 2019). Prequalified WHO cholera vaccines require more than one dose, but there is evidence that a single dose may offer modest protection (Azman et al., 2015). Scheduling difficulties with repeated vaccine administration visits lead to missed dosages and decreased immunity. Studies of Dukoral efficacy in Bangladesh saw lower efficacies in children between 2 and 5 years old and that simultaneous supplementation of zinc and vitamin A may be necessary to increase immune response (Albert et al., 2003). Current killed OCVs are not based on strains representative of current epidemic *V. cholerae* strains. Dukoral is only protective against the O1 serogroup and not against other serogroups (Sit et al., 2022). Dukoral must be administered with an

oral buffer, unlike Shanchol and mORC-vax, which can strain logistics in a disaster situation. The WHO has reported a global shortage of OCVs, which has forced a suspension of the 2 dose guidelines in favor of a single dose (*Cholera Vaccine Shortage Forces Shift to One-Dose Regimen*, 2022). Vaxchora production has been discontinued due to COVID-19 pandemic related reduction in international travel and is currently unavailable in the US (Research, 2022).

Live attenuated vaccines have significant advantage over killed OCVs in number of doses and potentially longevity of immunity. Live attenuated vaccines, such as Vaxchora, have shown very high rates of protection at 10 days and 3 months post administration compared to Dukoral (Saluja et al., 2019). Not only can OCVs with specific mutations increase immunogenicity, but they can also potentially offer rapid protection during an outbreak by competing and preventing colonization of pathogenic bacteria (Sit et al., 2019). Live attenuated OCV PanChol, formerly known as HaitiV, is a next generation live attenuated OCV based on the O1 El Tor Ogawa clinical isolate from Haiti in 2010, that contains deletions of the entire Ctx prophage as well as the RTX toxin and alpha-hemolysin. Furthermore, the vaccine strain is bivalent, expressing both Inaba and Ogawa serotypes conversion, through the same genetic mutation as Hillchol (Sit et al., 2022). To address biosafety concerns of toxigenic reversion, PanChol contains a CRISPR/Cas9 system which targets Ctx-A and deletion of the CTX phage attachment site (Hubbard et al., 2018). As of March 2023, PanChol is currently undergoing the dose escalation stage of a phase I clinical trial.

Currently there is no commercially available or WHO prequalified ETEC vaccine, however, there has been mounting investment in ETEC vaccines with multiple ongoing clinical trials. ACE527 is a new live ETEC vaccine which is a combination of genetically modified and attenuated ETEC strains and has been shown to protect against ETEC challenge in adult humans (Harro et al., 2019). There has also been some evidence of OCVs offering some protection against ETEC due to similarities in their AB<sub>5</sub> toxins (Song et al., 2021).

### ***Outer Membrane Vesicles and the Mla Pathway***

The outer membranes of Gram-negative bacteria are asymmetric in composition between the outer and inner leaflet: the outer leaflet is mainly composed of LPS and the inner leaflet largely contains phospholipids. Outer membrane vesicles (OMVs) are produced by all Gram-negative bacteria and are the product of outer membrane “pinching” of bulges of the outer membrane. OMVs display outer membrane proteins and LPS on their surface and can contain components of the periplasm, such as peptidoglycans, and cytoplasmic contents in the lumen. OMVs have several functions: adaptation to the environment, transportation of virulence factors, or response to stress (Jan, 2017). OMVs can also facilitate defense against antimicrobial agents. OMVs readily interact with epithelial and endothelial tissues and can induce an inflammatory response leading to dysregulation and atrophy of tissue. OMVs can have immunogenic and adjuvant capability (Tan et al., 2018). Specifically in pathogens of the gastrointestinal system, OMVs act as carriers for toxins either contained on the inside of the vesicle or extracellularly displayed

on the outer membrane. Both Ctx of toxigenic *V. cholerae* and ETEC heat labile enterotoxin have been associated with OMVs. The small size of OMVs, typically between 20 to 250 nm, allow them to maneuver into tissue compartments and pass through protective barriers. Mechanistically, increased production of OMVs helps to sequester membrane targeting antibiotics and antimicrobials, essentially acting as a decoy (Jan, 2017).

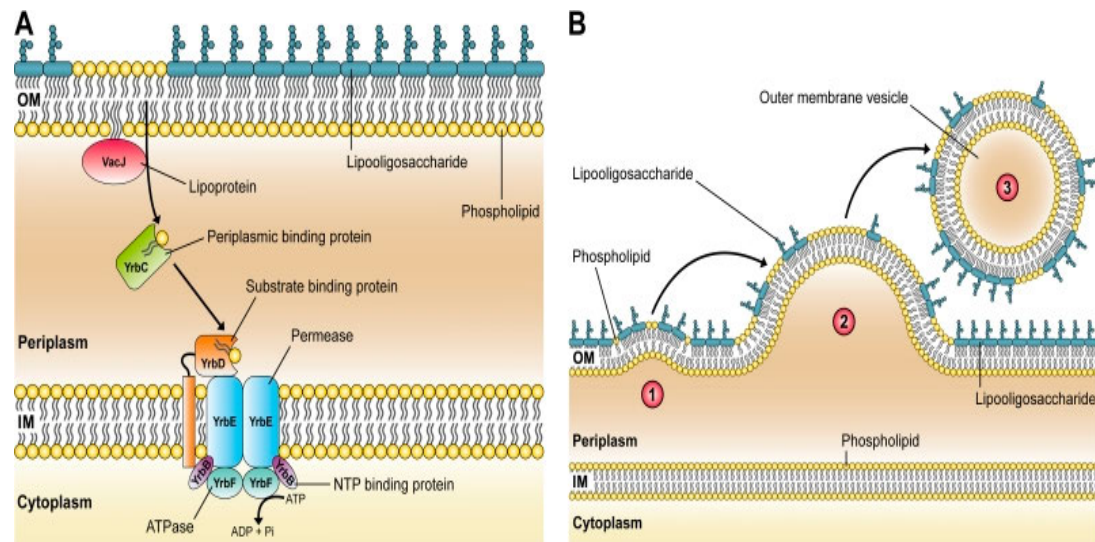


**Figure 1. OMV Biogenesis via the Mla pathway.** (A) Mechanism of Mla pathway utilizes shuttling of phospholipids through the VacJ/Yrb ABC (ATP-binding cassette) transport system from the outer leaflet of the outer membrane. (B) Scheme of OMV biogenesis from increased outer membrane asymmetry via the Mla pathway. Copyright disclaimer notice: the figure is comprised of unmodified Figure 1a and 8 from the original article (Roier et al., 2016), which is licensed under a Creative Commons Attribution 4.0 International License.

The mechanisms of OMV biogenesis, function, and structure vary. Models of OMV biogenesis include loss of linkages between the outer membrane and peptidoglycan in the periplasmic space, increased pressure on the outer membrane due to accumulation of misfolded proteins in the periplasmic space, and increased concavity of the outer membrane due to specific molecules which alter the curvature of the LPS layer (Jan, 2017).



OMV production is in part controlled by the Mla (VacJ/Yrb ABC (ATP-binding cassette) transport system. The genes required for this ABC transporter system are conserved across prokaryotes (Roier et al., 2016). The ABC transport system (cassette) is a core part of the Mla pathway which removes phospholipids from the outer leaflet of the outer membrane. The Mla pathway components are encoded by the following genes: *m1aA*, *m1aB*, *m1aC*, *m1aD*, *m1aE*, and *m1aF*. MlaB, -D, -E and -F are proteins which comprise the ABC transporter while MlaA and MlaC are periplasmic proteins. MlaA removes phospholipids from the outer leaflet of the outer membrane and MlaC is an associated shuttling molecule. The mechanism of the Mla pathway is thought to be as follows: phospholipids from the outer leaflet of the OM initiate phospholipid retrograde shuffling from the outer membrane to the ABC transporter in the inner membrane (Malinverni & Silhavy, 2009). MlaE is a permease and a critical component of the pathway (Linton & Higgins, 1998). Mutations in the Mla pathway lead to an increase in phospholipids in the outer leaflet of the OM. The increasing difference of phospholipid composition in the OM leads to bulging and OMV formation (Malinverni & Silhavy, 2009). Another factor that can lead to the downregulation of VacJ/Yrb ABC transport system is low iron (Roier et al., 2016). The composition of OMVs of transporter mutants compared to wild type can vary.  $\Delta m1aE$  mutants were shown to have an altered lipidome with a higher composition of phosphatidylethanolamine and a decrease in C16:0 FAs (Roier et al., 2016). In contrast, the protein composition was not impacted by transporter mutations. Mutations in *V. cholerae* ABC transporter of the Mla pathway showed a 4-fold increase in OMV production with similar results observed in *E. coli* (Zingl et al., 2020).

### ***OMV Vaccine Implications***

Recently there has been interest in harnessing hypervesiculation and OMVs as a strategy for vaccine development. Bexsero® is a commercially available OMV containing vaccine against *Neisseria meningitidis* with evidence of widespread effectiveness in all age groups (Petousis-Harris, 2017). OMVs can also act as non-specific immune potentiators, or adjuvants, which can promote immune responses (Tan et al., 2018). Studies of *E. coli* and *V. cholerae* OMVs in mouse infection models indicate OMVs can induce a robust immune response (Leitner et al., 2015). One advantage of OMVs over traditional adjuvants and vaccines is due to their ability to display antigens extracellularly as well as transport them intracellularly. Assimilation of OMVs across cell membranes imports antigens intracellularly (Tan et al., 2018). Because OMVs are non-living they provide a safe transportation vehicle of intact bacterial antigens with no risk of virulence reversion. OMVs of various species have been shown to stimulate dendritic cells, leading to production of anti-OMV specific antibodies and T cell activation (Alaniz et al., 2007). OMVs can display a diverse set of antigens and can activate a wide range of immune pathways (Lieberman, 2022). Because OMVs are produced by bacteria, their composition can be readily manipulated (Lieberman, 2022). Gram negative bacteria can be modified to hypervesiculate, combining additional benefits of OMV adjuvants to the proven protective ability of live attenuated vaccine.

## SPECIFIC AIMS

The current global cholera and ETEC situation necessitates the development and testing of improved vaccines, particularly for young children. New live attenuated OCVs to combat the growing morbidity and mortality of cholera and ETEC cases around the globe could be extremely beneficial as single dose agents for vaccination of all age groups. In my work, I investigated whether a hypervesiculating ETEC strain could be a platform for a future live attenuated vaccine. OMVs are immunogenic and have been shown to have adjuvant properties. Knockouts of the *Mla* pathway have been shown to increase OMV production in multiple enteric pathogens without diminishing their outer membrane integrity. I developed a suckling mouse model for investigation of ETEC pathogenicity and created a barcoded  $\Delta mlaE$  ETEC mutant library and compared its intestinal colonization dynamics to that of wild type (WT) ETEC through introduction of short random nucleotide sequences (barcodes) into the genome. I then used sequence tag-based analysis of microbial population dynamics (STAMPR) to examine the difference in founding population sizes. Furthermore, I participated in the ongoing first-in-human phase I clinical trial for the live attenuated OCV PanChol, by measuring the shedding and serotype of the vaccine strain in fecal samples from volunteers. Previous animal studies of PanChol have shown an induction of an immune response which confers robust cross-protection against both O1 serotypes. Further investigation of PanChol in a human clinical trial is necessary to understand its viability as an OCV.

This thesis seeks to achieve the following goals: comparison of OMV production between ETEC WT and mutant, the construction of barcoded ETEC libraries using

triparental mating with donor *E. coli* strains, establishment of a neonatal mouse ETEC infection model, determination of founding population and colonization of barcoded ETEC strains, and shedding of the next generation PanChol cholera vaccine.

## METHODS

### *Barcoding of ETEC*

The methods were previously described and adapted from Hullahalli et al., 2021. A triparental mating system was used to integrate  $5 \times 10^5$  barcodes present from MFD $\lambda$ pir pSM1 into ETEC recipient using molecular machinery from MFD $\lambda$ pir pJMP1039. Recipient strains (ETEC WT and  $\Delta mlaE$ ) and MFD $\lambda$ pir pJMP1039 were streaked on LB + 200 mg/mL streptomycin (Sm200) plates and incubated overnight at 37°C. Three mL overnight cultures of each donor and recipient in LB and appropriate antibiotics were made. MFD $\lambda$ pir pJMP1039 received 30  $\mu$ L of diaminopimelic acid (DAP) and 3  $\mu$ L of 100 mg/mL carbomycin (Carb). MFD $\lambda$ pir pSM1 received 30  $\mu$ L of DAP, 3  $\mu$ L of Carb and 3  $\mu$ L of 50 mg/mL kanamycin (Kan50). Recipients received 1 colony from either ETEC WT or  $\Delta mlaE$ , MFD $\lambda$ pir pJMP1039 received one line of colonies scraped from plates using a pipette tip and MFD $\lambda$ pir pSM1 received 30  $\mu$ L from a frozen stock. Overnight cultures were incubated on a Innova 210 platform shaker (New Brunswick Scientific) at 37° C and 250 rpm. 15 pools of 200  $\mu$ L of the recipient strain and 100  $\mu$ L of each donor strain were formed and were centrifuged for 5 min at 6,000 G at 25° C. The supernatant was decanted, and pellets were resuspended in 300  $\mu$ L LB. The solutions were centrifuged again at the previous setting. The supernatant was decanted, and the pellet was resuspended with 300  $\mu$ L of 1:10 DAP, LB solution. 100  $\mu$ L of the resuspended pellets were spotted onto 0.45  $\mu$ m filters on LB + DAP plates for a total of 45 filters on 9 plates which were incubated for 4 h at 37° C. 100  $\mu$ L of each recipient and donor culture was spotted on a separate filter as a control. After 4 h, the filters were

placed into 50 mL tubes with 6 filters each along with 2 mL phosphate buffered saline (PBS). The tubes with filters were then resuspended and vortexed until the solution was turbid and then 600  $\mu$ L was plated on large Sm200 + Kan100 plates. 10  $\mu$ L of residual solution was used for serial dilutions to enumerate transconjugants. All plates were incubated overnight at 37° C. 2 ml of 2:1 LB + glycerol solution was used to scrape lawns and the library was pooled into a 50 mL tube, vortexed until completely homogenous, aliquoted, and stored at -80° C.

The barcodes in the libraries were validated via formation of standard curve via serial dilution, which simulates a biological bottleneck. A cultured solution of 3 mL LB, 30  $\mu$ L of ETEC strain and 3  $\mu$ L of Sm200 was serially diluted 1:10 from undiluted down to 10<sup>-6</sup> twice. 100  $\mu$ L of each dilution was then plated onto LB + Sm200 plates for a total of 14 plates and incubated at 37° C for 18 hours. The plates were scraped with 1 ml of 2:1 LB glycerol solution. Sequencing was done via MiSeq (Illumina) and the analysis of barcodes was completed via methods described by Hullahulli et al., 2021. The amount of determined CFU from serial dilutions (simulated founding population) was compared against the number of barcodes to determine accuracy of founding population estimates.

### ***Pooled ETEC Library Formation***

LB + Sm200 agar plates were streaked using frozen barcoded ETEC stock. 15 overnight cultures were formed from distinct single colonies with Sm200 and incubated at 37° C. 600  $\mu$ L of glycerol was added to 1.8 mL cryotubes and then a pool of 400  $\mu$ L from 3 different cultures for a total volume of 1.8 mL. The 5 pooled samples were

vortexed, labeled, and frozen at -80° C. Analysis of pooled ETEC libraries was done through sequencing.

### ***Sequencing and STAMPR***

Briefly, 2  $\mu$ L of frozen library stock were added to 100  $\mu$ L of water and boiled at 95° C to lyse the cell. PCR of the boiled samples was performed to amplify the DNA needed for sequencing. Amplified products were run on a 1% agarose gel for validation of the barcoding process and presence of the amplicon. All the samples were then pooled, purified using the GeneJet PCR Purification Kit (Thermo Fischer Scientific), quantified via Invitrogen Qubit 2.0 fluorometer (Thermo Fischer Scientific) and sequenced with either a Miseq or Nextseq 1000 (Illumina) for 78 cycles. Further computational analysis of barcodes and founding population,  $N_s$ , via STAMPR is outlined in Hullahalli et al., 2021. The full code for genetic analysis can be found at [https://github.com/hullahalli/stampr\\_rtisan](https://github.com/hullahalli/stampr_rtisan).

### ***OMV Isolation***

ETEC WT and  $\Delta mlaE$  strains were streaked on LB + Sm200 plates and 4 colonies of each strain were used for single colony cultures with 3 mL LB and 3  $\mu$ L Sm. The overnight cultures of each strain were diluted 1:100 in LB and incubated in an Innova 42 shaker (New Brunswick) for 8 hours at 180 rpm and 37° C. OD<sub>600</sub> measurement and serial dilutions were used to enumerate growth. OD<sub>600</sub> measurement was taken using a 2 mL blank of LB and a 1:10 dilution of ETEC strains with LB for a total volume of 2 mL.

Serial dilutions from  $10^{-2}$  to  $10^{-7}$  were plated. The solutions were transferred to 50 mL tubes and centrifuged for 20 min at 7830 rpm at 4° C. The supernatant was filtered through a 0.22  $\mu$ m polyethersulfane (PES) filter. PES filters were changed every 100 mL of supernatant. 1 mL of filtrate is spotted on LB plates as a contamination check. The filtered supernatant was centrifuged using an Optima XE-90 Ultracentrifuge (Beckman Coulter) for 4 h at 6° C and 28,600 rpm. The supernatant was decanted, and pellets were dissolved in 60  $\mu$ L PBS and stored at -20° C.

### ***OMV Protein Concentration***

The concentration of OMVs produced by each strain was determined via Nanodrop ND-1000 spectrophotometer (Thermo-Fischer) measuring UV absorbance at 280 nm. The nanodrop was blanked with 2  $\mu$ L of PBS before use. OMV samples were thawed and vortexed before 2  $\mu$ L of each sample was added to the nanodrop.

### ***Neonatal Mouse ETEC Infection Model***

Overnight cultures of ETEC WT were prepared in 3 mL LB, 3  $\mu$ L Sm200 and 30  $\mu$ L of ETEC WT from frozen stock for 20 h. The OD<sub>600</sub> was measured, and then serial dilutions were made from 1:10, 1:100, 1:1000 dilutions in LB to yield  $10^7$ ,  $10^6$ ,  $10^5$  CFU, respectively. 10  $\mu$ L of diluted cultures was used to determine input CFU. The final infection mixture was formed by adding 5  $\mu$ L of green food dye (McCormick) to 1 mL of diluted culture. 5-day old (P5) C57BL/6 and CD-1 mice from Charles River Laboratories were orally administered with 50  $\mu$ L of the infection mixture and incubated for 20 h. The



mice were sacrificed using isoflurane, followed by decapitation. The small intestine (SI) was harvested and homogenized in 1 mL PBS. 10  $\mu$ L of the homogenized SI were serially diluted on LB + Sm200 plates from undiluted to  $10^{-6}$  level dilution to determine the ETEC CFU burden in the SI. Mice litters from different dams were mixed to control for possible litter effects.

### ***Dose Specific ETEC Colonization***

Neonatal mouse colonization of barcoded ETEC WT and barcoded  $\Delta mlaE$  followed similar methods as described above. Overnight cultures were made using 30  $\mu$ L of frozen barcoded ETEC libraries. The inocula of the barcoded libraries were approximately  $10^6$  and  $10^7$ , which were made via 1:100 dilution of overnight cultures of each library.  $10^5$  CFU/ml dosage was created by diluting overnight cultures 1:4 and then 1:1000 in another tube. 100  $\mu$ L of the inoculum culture was plated onto large LB + Sm200 plates for both barcoded libraries to determine barcode frequencies in the inocula. Following serial dilution of homogenized SI, the remaining volume was plated on LB + Sm200 plates to determine barcode frequencies in output. Founding population sizes were determined by comparing input and output barcodes via sequencing and STAMPR analysis.

### ***Growth Curve of ETEC Strains***

Cultures were prepared with ETEC WT and  $\Delta mlaE$  and their respective barcoded variants in 3 ml LB, 3  $\mu$ L Sm200 and approximately 20  $\mu$ L scrapped from frozen stocks.

Following a 16 h incubation period, the overnight cultures were diluted 1:1000 in LB with Sm200 and 200  $\mu$ L of each diluted culture was added to 20 wells on a 96 well plate. The 96 well plate was wrapped in parafilm and analyzed for 24 hours on Epoch 2 microplate spectrophotometer (Biotek) with OD<sub>600</sub> measurements taken every 10 minutes.

### ***Thiosulfate-Citrate-Bile Salts-Sucrose Agar (TCBS) Plates***

44g of TCBS agar powder (Sigma Aldrich) was added to a 500 mL volumetric flask with a stir bar along with 250 ml of deionized water. The agar was homogenized and then another 250 mL of water was added for a total volume of 500 mL. The TCBS agar solution was heated and stirred on a hot plate for 1 h at 180 degrees Celsius and 400 rpm. The solution was then microwaved for 2 minutes at power 7. The solution is then left to cool and an appropriate amount of Sm200 is added. The TCBS procedure was adapted and modified from the manufacturer's recommendation.

### ***Quantitative and Qualitative Analysis of PanChol***

Following the administration of PanChol, fecal samples were delivered when available by the clinical investigations unit of Brigham and Women's Hospital. 1 g of fecal sample was homogenized in 9 mL of PBS in a 50 mL tube, from which 1 mL of supernatant was added to a 1.5 mL Eppendorf tube. The fecal supernatant was then serially diluted from undiluted to 10<sup>-6</sup> and 100  $\mu$ L of each dilution was plated separately on both TCBS and LB + X-Gal Sm200 plates. In the absence of a fecal sample, a rectal

swab was streaked on both TCBS and LB + X-Gal Sm200 plates and incubated overnight.

### ***Serotyping of PanChol***

A colony taken from a fecal cultured plate was added to and resuspended in a PCR tube with 20  $\mu$ L of LB medium. 8  $\mu$ L of resuspended colony solution is spotted on a glass slide with 5  $\mu$ L of Difco™ *Vibrio Cholerae* antiserum Inaba or Ogawa (BD). The solutions were mixed with a pipette tip every 5 minutes for 20 minutes. A positive result was determined through the presence of white agglutinates.

### ***Statistical Analysis***

Graphical application Prism 9 (Graphpad) was used for statistical analysis of the samples with an unpaired 95% confidence interval t-test. P-value less than 0.05 was considered statistically significant. Geometric means were used to account for variability in data sets.

### ***Animal Use Statement***

All neonatal mice experiments were in compliance with the *Guide for Care and Use of Laboratory Animals* and were performed as approved by the Brigham and Women's Hospital IACUC (Protocol #2016N000416). Neonatal mice were euthanized through isoflurane inhalation followed by decapitation using a razor blade.

## RESULTS

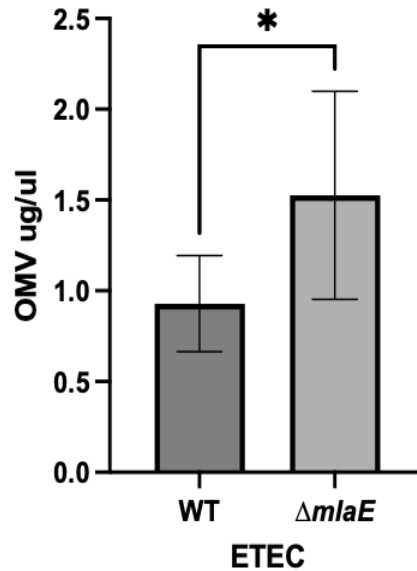


**Figure 2. Protein Concentration from OMV Isolates.** OMVs from non-barcoded ETEC strains were isolated through multiple rounds of ultracentrifugation and the samples' protein absorbance were measured using a nanodrop ND-1000 spectrophotometer at 280 nm. ETEC  $\Delta mlaE$  produced significantly more OMV proteins than the wild type ( $p < 0.05$ ).

To quantify OMV biogenesis in ETEC WT and  $\Delta mlaE$ , protein absorbance at 280 nm OMV samples was measured through a nanodrop spectrophotometer to determine OMV protein concentration. OMV samples of the mutant were significantly larger than the wild type ETEC ( $p < 0.05$ ). The ETEC  $\Delta mlaE$  mutant had higher variability with a larger standard deviation and interquartile range.

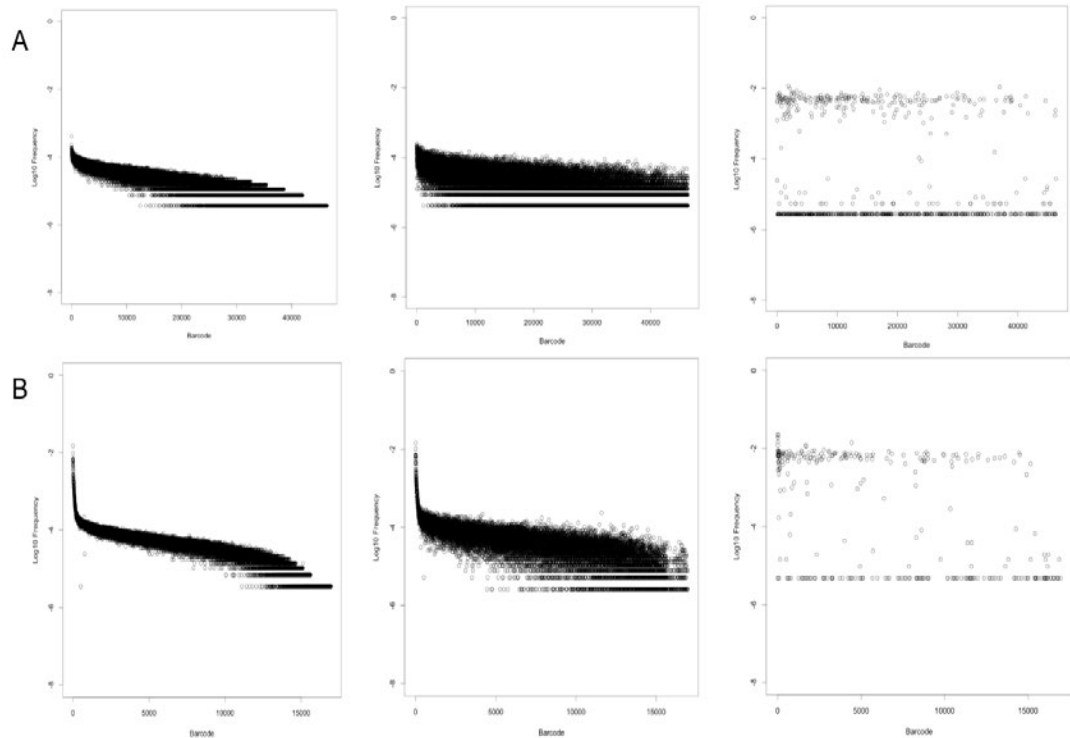


**Figure 3. Barcode Frequency distribution of ETEC Libraries at Different Dilutions.** Shown are the distribution of ETEC WT and  $\Delta mlaE$  barcodes in the dilutions at  $10^0$ ,  $10^{-3}$ ,  $10^{-6}$ , respectively for (A) ETEC  $\Delta mlaE$  library and (B) ETEC WT library. ETEC  $\Delta mlaE$  library contained approximately  $4 \times 10^4$  barcodes and the ETEC wild type library consisted of  $1.7 \times 10^4$  barcodes.

Triparental mating of *E. coli* donor strains MFD $\lambda$ pir pJMP1039 and MFD $\lambda$ pir pSM1 with ETEC recipients was used to form unpooled and pooled barcoded ETEC libraries for use in *in vitro* studies and animal infection models to understand founding population, bottleneck dynamics as well as colonization of ETEC strains. The unpooled ETEC transconjugant libraries were serially diluted, thereby creating known bottlenecks. Then, the CFU from the serial dilution plates were scraped and sequenced to test whether the libraries could be used to accurately determine founding population by plotting a standard curve. These analyses showed that there was similar distribution of barcodes in

the unpooled libraries, i.e., there were no highly represented barcodes (Fig. 4). The pooled libraries each had 3 overrepresented, distinct barcodes (Fig. 5).

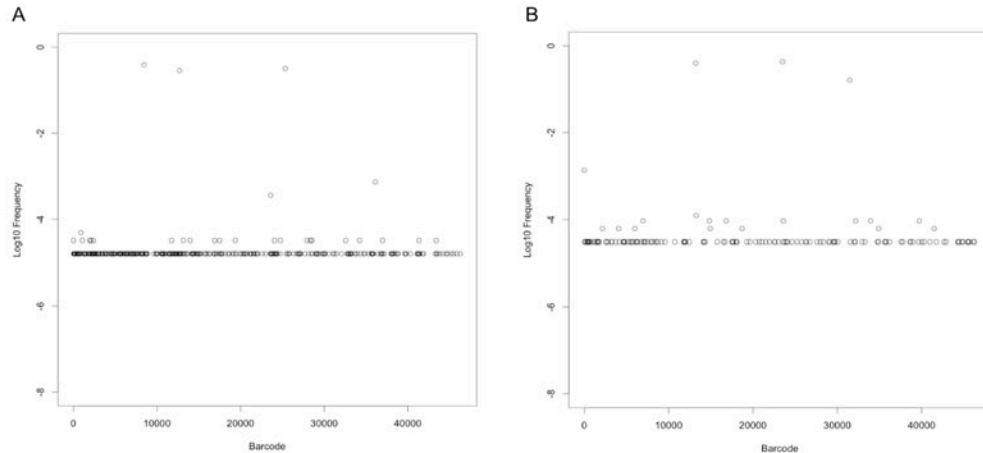


**Figure 4. Raw Barcode Reads of ETEC Pooled Libraries.** (A) ETEC WT BC and (B) ETEC  $\Delta mlaE$  BC pooled libraries display 3 distinct barcodes at high frequency with low background.

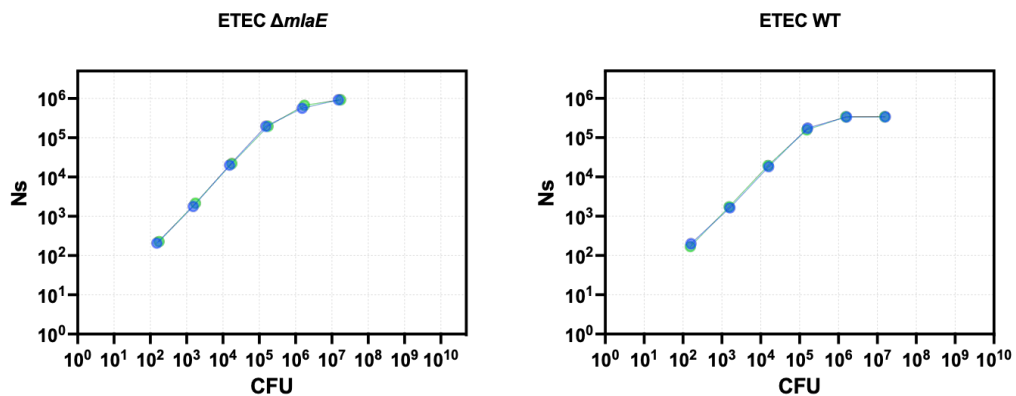


**Figure 5. In vitro STAMPR standard curves of barcoded ETEC strains.** Calibration curves of the ETEC strains were determined by plotting observed CFU on plates from serial dilutions of the library (CFU) plotted against the number of distinct barcodes ( $N_s$ ) which represents the estimated bottle neck. Blue and green lines are data of the same strain from duplicate samples.

The total number of barcodes in the unpooled library for ETEC WT was  $1.7 \times 10^4$ , compared to  $4.6 \times 10^4$  for ETEC  $\Delta mlaE$ . The standard curves revealed that the libraries had a linear relationship up to  $\sim 10^6$  for the mutant and up to  $10^5$  for the wild type (Fig. 6),

indicating that these libraries have a robust, dynamic range for determination of bottleneck sizes.

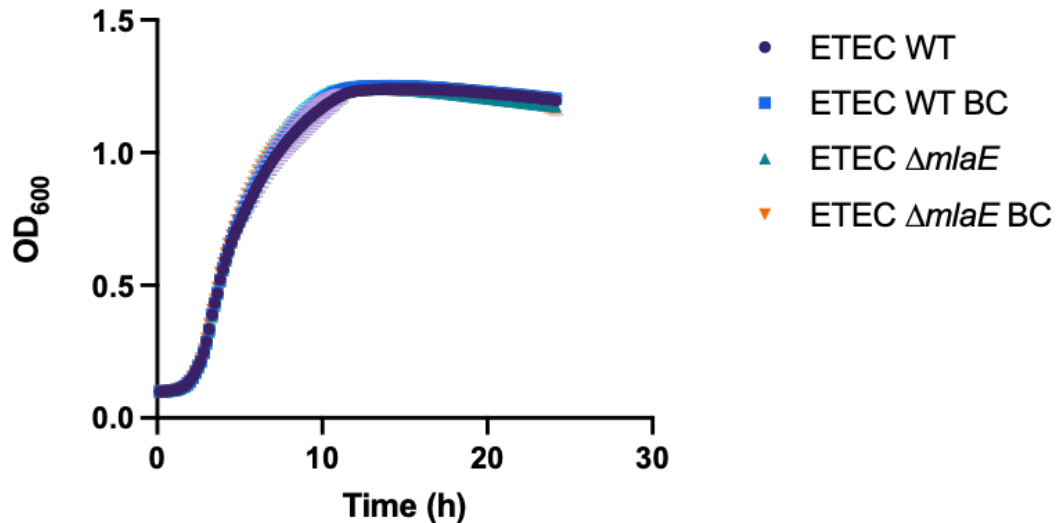


**Figure 6. Growth Curve of barcoded and non-barcoded ETEC strains.** The growth of the tagged and untagged ETEC strains were largely indistinguishable with slight variation during the exponential growth phase between 7 and 12 h, indicating that the introduction of the barcodes did not confer any changes in growth.

To see if the introduction of the barcodes impacted growth, a growth curve was determined by comparing each ETEC strain and their respective barcoded variants through OD<sub>600</sub> measurements of cultures every 10 minutes for 24 hours. There was no significant difference in growth between ETEC WT strains and their barcoded derivatives (Fig. 7).

ETEC H10407 neonatal mice infection models have not been systematically described, although a wide range of mouse ages and strains have been used. To determine the optimal mouse strain and dosage of bacteria for an infection model, the commonly

used outbred CD-1 mice was tested along with the inbred strain C57BL/6, which is the strain often used for creation of genetically engineered mice.

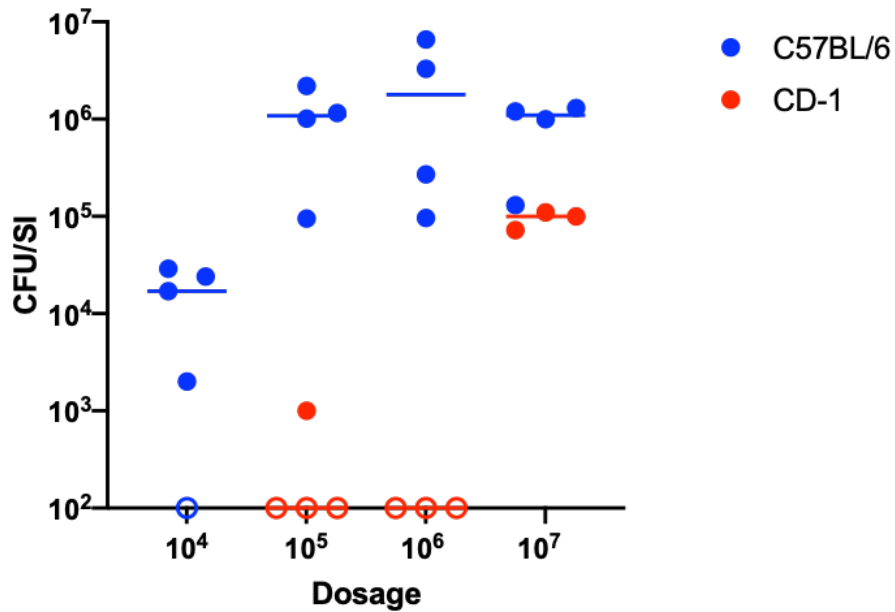


**Figure 7. ETEC WT colonization in P5 neonatal mice.** C57BL/6 and CD-1 mice were inoculated with varying doses of ETEC WT and sacrificed following 20 hours post inoculation. Open circles at  $10^2$  CFU/SI represent values below limit of detection of the assay. Colonization per SI from inocula ranging from  $10^5$  to  $10^7$  were comparable and statistically different from  $10^4$ . Little colonization was observed in CD-1 mice below an inoculum of  $10^7$ .

The dosage range tested was approximately  $10^4$  to  $10^7$  CFU for C57BL/6 and  $10^5$  to  $10^7$  for CD-1 mice. In C57BL/6 mice, there was a significant difference in ETEC WT SI colonization between  $10^4$  and every other dose tested ( $p < 0.05$ ), but colonization at inocula sizes of  $10^5$  to  $10^7$  were comparable ( $p > 0.05$ ) (Fig. 8). Other than an outlier at  $10^5$ , only doses of  $10^7$  CFU/mL routinely led to colonization greater than the limit of detection in CD-1 mice, suggesting that the inbred mouse strain has a wider more permissive bottleneck than the outbred CD-1 animals (Fig. 8).



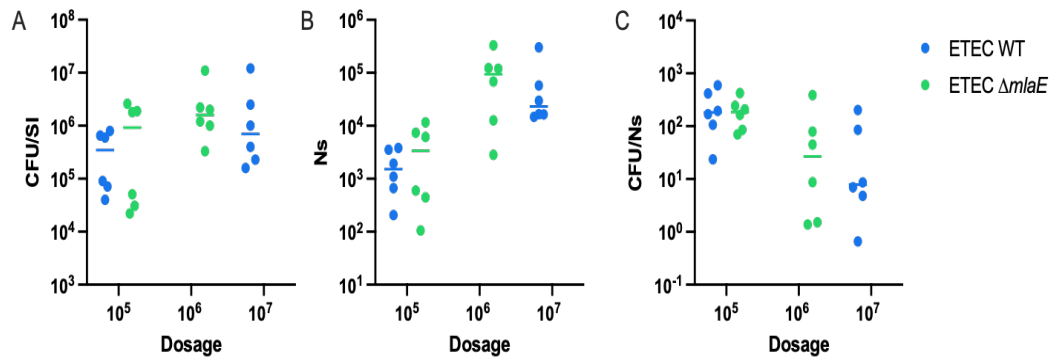


**Figure 8: Colonization and founding population of barcoded WT and  $\Delta mlaE$  ETEC.** P5 C57BL/6 mice were orally infected with barcoded ETEC strains at varying doses to determine whether an increase of OMV biogenesis leads to an increase in colonization, founding population or clonal expansion. (A) An input of approximately  $6.5 \times 10^5$  CFU/mL yielded no significant difference in in vivo growth between ETEC strains. ETEC WT colonization with an input of  $10^7$  was comparable to the mutant with 10-fold less dosage. (B) The founding population (Ns) of both ETEC wild type and the  $\Delta mlaE$  was approximately  $10^3$  at an input of  $10^5$  and increased with input size. (C) The clonal expansion was 165 CFU/Ns for both ETEC strains at  $10^5$  inoculum, but CFU/Ns decreased as the input increased.

Using the neonatal mouse infection model with P5 C57BL/6 mice, ETEC WT and  $\Delta mlaE$  BC were compared at varying infection dosages to investigate if an increased production of OMVs influences colonization or founding population sizes. An inoculum of approximately  $6.5 \times 10^5$  yielded similar SI colonization in ETEC WT and  $\Delta mlaE$  (Fig. 9). There was no significant difference in colonization between the mutant and wild type even though the mutant was infected with 10-fold less bacteria. Colonization at  $10^6$  and  $10^7$  was greater than at  $10^5$ , however, the difference was not significant. Clustering of the colonization data into two groups was observed in mice given  $10^5$  mutant or wild type and the range in the groups were 10-fold and 100-fold, respectively (Fig. 9).

The founding population of both ETEC strains following an input of  $10^5$  was approximately  $1.3 \times 10^3$  and the expansion of the founding population between ETEC

strains was almost identical at 165 CFU/Ns (Fig. 9C). Interestingly, there is a wide range of founding populations in both ETEC strains; the  $\Delta mlaE$  founding population range was 10 to 100-fold wider compared to the wild type (Fig. 9B). At an input of  $5.5 \times 10^5$ , the data suggests that the host bottleneck causes a  $10^2$ -fold reduction in both ETEC strains which expands back to the size of the original inoculum. The founding population increased as the dosage increased in both ETEC strains, however, the clonal expansion of the founding population decreased as the dosage increased (Fig. 9).

PanChol is a next generation OCV which includes alterations that have been shown to elicit rapid protection as well as cross protection of serotypes in mice models (Sit et al., 2019). As of spring 2023, the OCV is currently in a phase I clinical trial to determine toxicity, preliminary efficacy in humans (measured by its immunogenicity), dosage and side effects. The clinical trial of PanChol also presents an opportunity to determine how colonization of this attenuated *V. cholerae* strain influences the composition of the microbiota. PanChol shedding was determined by plating serial dilutions of fecal samples from the volunteers. In the absence of available fecal samples, a rectal swab was used instead to qualitatively determine PanChol shedding in fecal samples. Volunteers 001 and 002 were both females under the age of 25. Volunteer 003 was a male over the age of 40. No volunteers experienced adverse symptoms and no stool samples were characterized as diarrhea. The average dosage of PanChol for the three volunteers was  $1.02 \times 10^6$  CFU/100 ml, which was very close to the intended  $10^6$  CFU/mL dose. This represents the first dose tier in this dose escalation study.

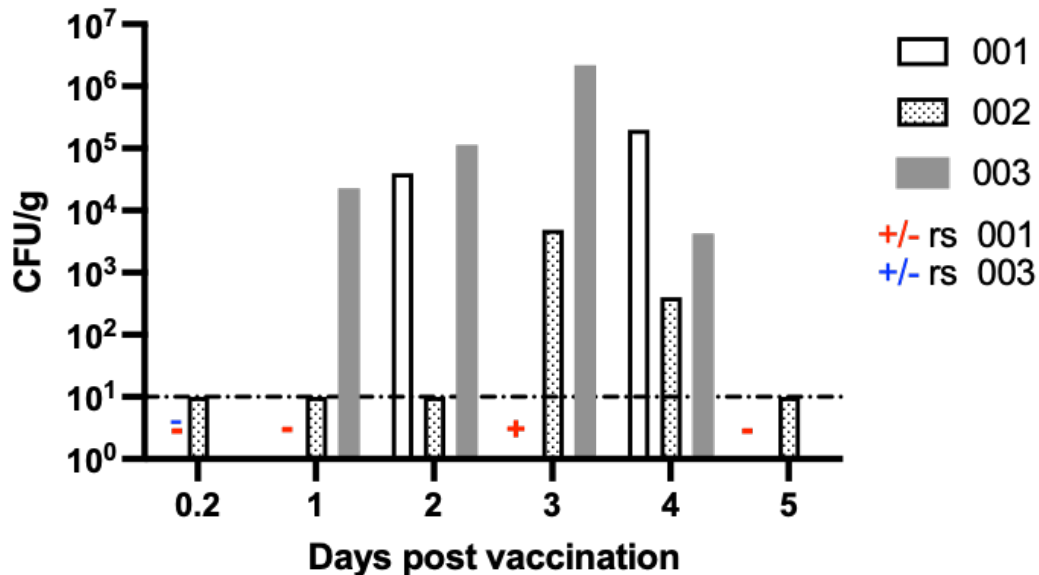


**Figure 9. Stool shedding of PanChol in Human Subjects.** OCV PanChol colonization in three volunteers: 001, 002, 003 following administration of  $10^6$  CFU was enumerated from fecal samples plated on TCBS agar plates. In the absence of fecal, rectal swabs (rs) were used to qualitatively determine the presence of PanChol in stool samples; rectal swabs were used in volunteers 001 and 003. Shedding of PanChol occurs begins ~24 h after administration with shedding at day 3-4, followed by a quick decline.  $10^1$  represents the limit of detection.

Colonization of PanChol in human subjects increased over the course of 72 hours post administration and then sharply declined. Patient 001 only had 2 fecal samples with a CFU/g of  $3.98 \times 10^4$  and  $2 \times 10^5$  on days 2 and 4, respectively (Fig. 11). Due to the absence of a fecal sample on day 3, it is unknown if maximum colonization was on day 3 or 4. Volunteer 002 provided fecal samples for all 5 days, thus a fecal swab was not taken. Analysis of fecal samples from volunteer 002 showed no colonization until day 3 and 4 which had a CFU/g of  $4.90 \times 10^3$  and  $4.00 \times 10^2$ , respectively (Fig. 11). Volunteer 003 had the most colonization of the three volunteers over the entire time course (Fig. 11). No sample, rectal swab or fecal sample, was produced on day 5 for volunteer 003.

An interesting qualitative finding was the appearance of streptomycin resistant bacteria in two of the subject's stools which led to blue background on LB + X-Gal Sm200 plates. A decrease in the number of colonies formed on LB + X-Gal compared to TCBS agar led to CFU determination was done with data from TCBS plates. The identity of the blue background has not been determined.

*V. cholerae* can change its serotype from Ogawa to Inaba based on the activity of the WbeT methyltransferase which methylates the O-antigen of LPS (Karlsson et al., 2016). Specific serotypes have been shown to have varying immunogenic responses. Serotyping of the Panchol during the time course of the experiment was used to ensure O-antigen stability following passage through the human gut microbiome. Determination of serotype utilizes anti O-antigen antibodies specific for Ogawa and Inaba, but not the Hikojima serotype as it displays both unmethylated and methylated LPS. An indication of Hikojima serotype is a positive Ogawa and Inaba test. Shedding from all volunteers were positive for both Ogawa and Inaba.

## DISCUSSION

### *OMV Amounts in Wild type and Mutant ETEC*

Protein concentrations were measured as a method of analyzing the concentration of OMVs produced. Controls indicated that there was no bacterial contamination of the OMV isolates which could have confounded the results. Our data on OMV biogenesis shares similarities and differences with other findings of *E. coli* and *V. cholerae*  $\Delta mlaE$  OMV biogenesis studies. Previous studies in ETEC OMV biogenesis saw approximately 3 times more OMVs produced by a MlaE deficient strain compared to the wild type (Roier et al., 2016). I found that the amount of OMVs produced in both the mutant and the wild type were less than reported (Roier et al., 2016) but I did observe the trend that the mutant produced more OMV than the WT. Both ETEC WT and  $\Delta mlaE$  had large ranges and variability of OMV protein concentration. In Zingl et al., 2020, similar experiments were conducted in wild type *V. cholerae* and there was an observed significant increase in OMV amounts in the  $\Delta mlaE$  mutant, which produced 1.6 times more proteins than the wild type. The amount of OMVs in *V. cholerae* was far greater compared to what was observed in both ETEC strains; this is likely due to differences in OMV production in different bacterial species, a topic worthy of further exploration. Defining the species determinants of OMV production could shed light on the general processes that control OMV production.

### ***Barcoding and STAMPR Analysis of ETEC Strains***

The growth curve of the barcoded strains of ETEC revealed that the inclusion of the barcodes and the deletion of *mlaE* does not impede growth. This is as expected as the barcodes are non-coding and are inserted into a neutral locus on the chromosome. The standard curves (Fig. 6) of the barcoded libraries served as a confirmation that the abundances of barcodes accurately reflects founding population sizes. The standard curve of wild type and mutant were comparable and sequencing of dilutions of the barcoded libraries (simulated bottleneck) showed that the founding population ( $N_s$ ) accurately reflects a founding population up to  $10^6$  in the mutant strain and  $5 \times 10^5$  in wild type, which is comparable to other STAMPR libraries (Hullahalli et al., 2021). Barcode frequency distributions of both ETEC strains showed low background and little noise.

### ***Neonatal Mouse Model of Infection with ETEC***

Our data revealed that ETEC WT H10407 has very different capacity to colonize the small intestines of neonatal mice. The prototypical ETEC strain did not robustly colonize the SI of neonatal CD-1 mice and only doses of  $10^7$  yielded any colonies above the limit of detection. Allen et al., described a linear relationship with inputs  $10^2$  to  $10^7$  CFU/mL in 3- to 8-week-old C57BL/6 mice. In sharp contrast, we found in P5 C57/BL/6 colonization of the SI plateaued at approximately  $10^6$  CFU at inoculum doses greater than or equal to  $10^5$  CFU/mL. This colonization plateau likely represents the carrying capacity of the SI for this pathogen. Interestingly the carrying capacity of the SI for *V.*

*cholerae* is more than ten times higher, suggesting that ETEC has a lower capacity to survive and proliferate in this organ.

In contrast to other mouse models, we have found that inbred mouse infection with ETEC resulted in neither mortality nor detrimental symptoms. C57BL/6 mice infected with  $10^5$  and  $10^3$  CFU have been previously shown to have a mortality rate of 21% and 6%, respectively (Duchet-Suchaux et al., 1990). None of our CD-1 or C57BL/6 mice had any diarrheal or adverse symptoms post 20 hours. One difference in the mortality rate and colonization between our findings and the literature may be due to the length of infection. We conclude that inbred C57BL/6 neonatal mice are a useful platform for the study of ETEC pathogenesis at dosages from  $10^5$  to  $10^7$ . Neonatal mouse models have certain advantages over the use of adult mice. Adult laboratory mice are not readily susceptible to enteric infections by *V. Cholerae* and ETEC and require administration of streptomycin prior to infection. Use of antibiotics reduce the microbiota burden in the intestinal tract and impact murine physiology. Mice administered broad spectrum antibiotics have morphological changes in the gastrointestinal tract and extra intestinal organs as well as the immune system (Kennedy et al., 2018). Streptomycin may allow for proliferation and virulence of enteric pathogens, but “germ free” invariably leads to modification of host physiology, which impacts the model’s ability to mirror infection in humans. In contrast, neonatal mice do not need to be pre-treated with antibiotics, as shown, and offer a cost-effective alternative to adults. Possible downsides of infant mouse models are the immaturity of the immune system and microbiota. Our neonatal mice infection model presents a novel methodology which can lead to robust

colonization at varying doses with no adverse symptoms within a short 20-hour infection window.

### ***Founding Population and Colonization of Barcoded ETEC Strains***

STAMPR analysis revealed that the hypervesiculation  $\Delta mlaE$  mutation does not significantly impact colonization or founding population, compared to the wild type in inbred neonatal mice. The founding population of both ETEC strains experienced a wide range with a  $10^5$  inoculum which may indicate variability in host bottlenecks, though in general, the bottlenecks have been wide in comparison to some bacterial founding populations which can be as small as a few individual cells (Campbell et al., 2023). The neonatal mouse bottleneck of ETEC leads to an approximate 100-fold reduction in the number of barcodes in the inoculum. Our finding of a positive relationship between founding population size and inoculum size has previously been observed in *V. cholerae* and other enteropathogens, such as *C. rodentium* (Campbell et al., 2023). An interesting observation was that the  $\Delta mlaE$  mutant had a greater increase in founding population compared to wild type ETEC at a 10-fold smaller dosage, potentially indicating that OMVs may impact the pathogen's ability to resist bottleneck, however, direct comparison at increasing inputs is necessary to understand both the mechanism of bottleneck and the impact of hypervesiculation. A decrease in clonal expansion in both ETEC strains as both dosage and founding population increased can be explained by the finite carrying capacity of the small intestine which limits proliferation.



### ***PanChol Shedding and Stability***

We found that PanChol shedding occurred at the lowest dosage of  $10^6$  CFU/mL. In comparison to CVD 103-HgR (Vaxchora), safety and immunogenicity studies from human volunteers in Maryland, shedding was only seen in 11% of vaccinees at a dose of  $\sim 4.4 \times 10^8$  CFU (Chen et al., 2014). Analysis of fecal samples has suggested that PanChol rapidly proliferates from the limit of detection to  $\sim 10^4$  CFU within 24 h, however the time course of the proliferation varies. An interesting observation was that this phenomenon occurs at different time points post vaccine administration, a range of 24 to 72 hours. Patient 002 had the longest incubation time and was the only subject to have colonies were streptomycin resistant which were not *V. Cholerae*. It is possible that these bacteria acted as a direct competitor to PanChol, occupying the same niches in the small intestine. Asymptomatic cholera infections feces usually contain approximately  $10^3$  CFU/g while severe infections (rice water diarrhea) can have  $10^{10}$  to  $10^{12}$  CFU/L, indicating that PanChol colonization is within range of WT *V. cholerae* colonization. A comparison of PanChol to Vaxchora and virulent *V. cholerae* shedding indicates that PanChol colonizes robustly at a dose lower than what is currently administered for Vaxchora, although it is currently unknown whether  $10^6$  CFU yields acceptable immunogenic response for short-term or long-term protection. Given the general correlation between shedding/colonization and immunogenicity, the current shedding is encouraging.

Serotyping indicated that the genetic modifications of PanChol did not affect the activity of the WbeT methyltransferase and the Hikojima serotype was retained in human

subjects. In previous studies, it has been shown that the serogroup of *V. Cholerae* may change via various environmental cues as well as during infection. Investigation of Haiti *V. Cholerae* O1 in Haiti during the 2015 outbreak showed a shift from Ogawa to Inaba over the course of 5 years due to multiple mutations in the *wbeT* gene (Alam et al., 2016). It was hypothesized that the change was a mechanism to evade anti Ogawa host immune responses. Mouse models have shown that there is a difference in immune response to Ogawa or Inaba based on vaccine serotype. Because the level of immune response can be influenced by the serotype, retention of the O-antigen structure in PanChol is critical to prevent variable protection and to account for possible changes in serotypes in future pandemic strains.

### ***Limitations***

Though protein concentrations were measured for OMV isolates, further methods of OMV quantification could give a more holistic picture of OMV biogenesis. Like the Nanodrop, the Bradford Assay measures protein concentration, but because the reagents in the Bradford Assay interact with a wider range of amino acids, it can be more accurate as the nanodrop which relies on aromatic amino acids. Purpald assay is used to measure the concentration of KDO, a component of LPS, and can confirm the presence of OMVs, as OMV isolates may contain excreted proteins in conjunction with OMVs.

The immune response to wild type and mutant ETEC was not explored and fitness of the mutant in comparison to the wild type was also not investigated. The difference in

barcodes found in the input in the bottleneck colonization experiment could possibly influence the results of the analysis of the founding population of ETEC strains.

Colonization, adverse symptoms, serotype stability in the human GI tract is currently unknown at doses greater than  $10^6$  as the dose escalation phase of the study is ongoing in March 2023. Low number of human subjects as well as absence of daily fecal samples make it difficult to determine the time course of PanChol colonization/shedding. Fecal swabs were sometimes used due to the absence of fecal samples; these swabs are only a qualitative method to indicate presence or absence of PanChol, but do not provide quantitative insight into colonization. In the absence of STAMP for PanChol, we are left without data regarding the founding population and bottleneck in human subjects and must rely on mouse models.

### ***Future Directions and Implications for Further Research***

Future investigations into ETEC  $\Delta mlaE$  include a competitive index (CI) of barcoded ETEC WT and  $\Delta mlaE$  BC via the pooled libraries in *in vivo* and *in vitro* to investigate whether an increase of OMV biogenesis leads to a fitness advantage in the same environment. In general, our developed C57BL/6 model could be valuable for future studies of ETEC pathogenesis. For example, Tn-Seq studies to define colonization determinants may be possible with this system. The establishment of an infant mouse model for ETEC can be further used for immunization studies. Fakoya et al. 2022, inoculated adult female C57BL/6 mice with an earlier iteration of PanChol. Upon immunization, the adult females delivered antibodies to pups via breast milk and the neonatal mice were challenged with *V. Cholerae* to determine immunogenic efficacy.

The described methodology can be applied in the same manner with ETEC WT and *ΔmlaE*.

Future plans necessary to determine efficacy of PanChol include expansion to a double blinded challenge study with WT *V. cholerae*. Analysis of PanChol immune response via vibriocidal titer assay and IgA quantification is ongoing. Another avenue of future research is the investigation of the impacts of PanChol on intestinal microbiota due to the proliferation of the vaccine in the GI tract of subjects. Further iterations of PanChol with the *ΔmlaE* mutation are in development. Given current preclinical and clinical data on PanChol, a future novel direction would be the development of a dual protection OCV by importing ETEC antigens into PanChol *ΔmlaE*.

**BIBLIOGRAPHY**

- Abel, S., Abel zur Wiesch, P., Davis, B. M., & Waldor, M. K. (2015). Analysis of Bottlenecks in Experimental Models of Infection. *PLoS Pathogens*, *11*(6), e1004823. <https://doi.org/10.1371/journal.ppat.1004823>
- Abel, S., zur Wiesch, P. A., Chang, H.-H., Davis, B. M., Lipsitch, M., & Waldor, M. K. (2015). STAMP: Sequence tag-based analysis of microbial population dynamics. *Nature Methods*, *12*(3), 223–226. <https://doi.org/10.1038/nmeth.3253>
- Alaniz, R. C., Deatherage, B. L., Lara, J. C., & Cookson, B. T. (2007). Membrane Vesicles Are Immunogenic Facsimiles of Salmonella typhimurium That Potently Activate Dendritic Cells, Prime B and T Cell Responses, and Stimulate Protective Immunity In Vivo. *The Journal of Immunology*, *179*(11), 7692–7701. <https://doi.org/10.4049/jimmunol.179.11.7692>
- Albert, M. J., Qadri, F., Wahed, M. A., Ahmed, T., Rahman, A. S. M. H., Ahmed, F., Bhuiyan, N. A., Zaman, K., Baqui, A. H., Clemens, J. D., & Black, R. E. (2003). Supplementation with zinc, but not vitamin A, improves seroconversion to vibriocidal antibody in children given an oral cholera vaccine. *The Journal of Infectious Diseases*, *187*(6), 909–913. <https://doi.org/10.1086/368132>
- Ali, M., Emch, M., Park, J. K., Yunus, M., & Clemens, J. (2011). Natural Cholera Infection–Derived Immunity in an Endemic Setting. *The Journal of Infectious Diseases*, *204*(6), 912–918. <https://doi.org/10.1093/infdis/jir416>
- Allen, K. P., Randolph, M. M., & Fleckenstein, J. M. (2006). Importance of Heat-Labile Enterotoxin in Colonization of the Adult Mouse Small Intestine by Human Enterotoxigenic Escherichia coli Strains. *Infection and Immunity*, *74*(2), 869–875. <https://doi.org/10.1128/IAI.74.2.869-875.2006>
- Anderson, J. D., Bagamian, K. H., Muhib, F., Amaya, M. P., Laytner, L. A., Wierzba, T., & Rheingans, R. (2019). Burden of enterotoxigenic Escherichia coli and shigella non-fatal diarrhoeal infections in 79 low-income and lower middle-income countries: A modelling analysis. *The Lancet. Global Health*, *7*(3), e321–e330. [https://doi.org/10.1016/S2214-109X\(18\)30483-2](https://doi.org/10.1016/S2214-109X(18)30483-2)
- Azman, A. S., Luquero, F. J., Ciglenecki, I., Grais, R. F., Sack, D. A., & Lessler, J. (2015). The Impact of a One-Dose versus Two-Dose Oral Cholera Vaccine Regimen in Outbreak Settings: A Modeling Study. *PLoS Medicine*, *12*(8), e1001867. <https://doi.org/10.1371/journal.pmed.1001867>

- Azman, A. S., Rudolph, K. E., Cummings, D. A. T., & Lessler, J. (2013). The incubation period of cholera: A systematic review. *The Journal of Infection*, *66*(5), 432–438. <https://doi.org/10.1016/j.jinf.2012.11.013>
- Beddoe, T., Paton, A. W., Le Nours, J., Rossjohn, J., & Paton, J. C. (2010). Structure, Biological Functions and Applications of the AB5 Toxins. *Trends in Biochemical Sciences*, *35*(7), 411–418. <https://doi.org/10.1016/j.tibs.2010.02.003>
- Belkaid, Y., & Hand, T. (2014). Role of the Microbiota in Immunity and inflammation. *Cell*, *157*(1), 121–141. <https://doi.org/10.1016/j.cell.2014.03.011>
- Bhuiyan, T. R., Lundin, S. B., Khan, A. I., Lundgren, A., Harris, J. B., Calderwood, S. B., & Qadri, F. (2009). Cholera Caused by *Vibrio cholerae* O1 Induces T-Cell Responses in the Circulation. *Infection and Immunity*, *77*(5), 1888–1893. <https://doi.org/10.1128/IAI.01101-08>
- Bragança Lima, M. V., Hinderaker, S. G., Ogundipe, O. F., Owiti, P. O., Kadai, B., & Maikere, J. (2021). Association between cholera treatment outcome and nutritional status in children aged 2–4 years in Nigeria. *Public Health Action*, *11*(2), 80–84. <https://doi.org/10.5588/pha.20.0078>
- Campbell, I. W., Hullahalli, K., Turner, J. R., & Waldor, M. K. (2023). Quantitative dose-response analysis untangles host bottlenecks to enteric infection. *Nature Communications*, *14*(1), Article 1. <https://doi.org/10.1038/s41467-023-36162-3>
- Cecil, J. D., Sirisaengtaksin, N., O'Brien-Simpson, N. M., & Krachler, A. M. (2019). Outer Membrane Vesicle—Host Cell Interactions. *Microbiology Spectrum*, *7*(1), 10.1128/microbiolspec.PSIB-0001–2018. <https://doi.org/10.1128/microbiolspec.PSIB-0001-2018>
- Chakraborty, S., Harro, C., DeNearing, B., Ram, M., Feller, A., Cage, A., Bauers, N., Bourgeois, A. L., Walker, R., & Sack, D. A. (2016). Characterization of Mucosal Immune Responses to Enterotoxigenic *Escherichia coli* Vaccine Antigens in a Human Challenge Model: Response Profiles after Primary Infection and Homologous Rechallenge with Strain H10407. *Clinical and Vaccine Immunology*, *23*(1), 55–64. <https://doi.org/10.1128/CVI.00617-15>
- Chen, W. H., Greenberg, R. N., Pasetti, M. F., Livio, S., Lock, M., Gurwith, M., & Levine, M. M. (2014). Safety and Immunogenicity of Single-Dose Live Oral Cholera Vaccine Strain CVD 103-HgR, Prepared from New Master and Working Cell Banks. *Clinical and Vaccine Immunology : CVI*, *21*(1), 66–73. <https://doi.org/10.1128/CVI.00601-13>
- Cholera*. (n.d.). Retrieved March 1, 2023, from <https://www.who.int/news-room/fact-sheets/detail/cholera>

- Cholera – Global situation.* (n.d.). Retrieved March 1, 2023, from <https://www.who.int/emergencies/disease-outbreak-news/item/2023-DON437>
- Cholera vaccine shortage forces shift to one-dose regimen.* (2022, October 19). <https://news.un.org/en/story/2022/10/1129672>
- Cholera—Malawi.* (n.d.). Retrieved March 1, 2023, from <https://www.who.int/emergencies/disease-outbreak-news/item/2022-DON435>
- Craig, L., Pique, M. E., & Tainer, J. A. (2004). Type IV pilus structure and bacterial pathogenicity. *Nature Reviews Microbiology*, 2(5), Article 5. <https://doi.org/10.1038/nrmicro885>
- di Tommaso, A., de Magistris, M. T., Bugnoli, M., Marsili, I., Rappuoli, R., & Abrignani, S. (1994). Formaldehyde treatment of proteins can constrain presentation to T cells by limiting antigen processing. *Infection and Immunity*, 62(5), 1830–1834.
- Duchet-Suchaux, M., Le Maitre, C., & Bertin, A. (1990). Differences in susceptibility of inbred and outbred infant mice to enterotoxigenic *Escherichia coli* of bovine, porcine and human origin. *Journal of Medical Microbiology*, 31(3), 185–190. <https://doi.org/10.1099/00221317-31-3-185>
- Enterobacteriaceae—ClinicalKey.* (n.d.). Retrieved March 3, 2023, from <https://www.clinicalkey.com/#!/content/book/3-s2.0-B9780323482554002186>
- Fakoya, B., Hullahalli, K., Rubin, D. H. F., Leitner, D. R., Chilengi, R., Sack, D. A., & Waldor, M. K. (n.d.). Nontoxicogenic *Vibrio cholerae* Challenge Strains for Evaluating Vaccine Efficacy and Inferring Mechanisms of Protection. *MBio*, 13(2), e00539-22. <https://doi.org/10.1128/mbio.00539-22>
- Garrigues, S., Kun, R. S., & de Vries, R. P. (2021). Genetic barcodes allow traceability of CRISPR/Cas9-derived *Aspergillus niger* strains without affecting their fitness. *Current Genetics*, 67(4), 673–684. <https://doi.org/10.1007/s00294-021-01164-5>
- Goldhar, J., Zilberberg, A., & Ofek, I. (1986). Infant mouse model of adherence and colonization of intestinal tissues by enterotoxigenic strains of *Escherichia coli* isolated from humans. *Infection and Immunity*, 52(1), 205–208.
- Gonzales-Siles, L., & Sjöling, Å. (2016). The different ecological niches of enterotoxigenic *Escherichia coli*. *Environmental Microbiology*, 18(3), 741–751. <https://doi.org/10.1111/1462-2920.13106>
- Harris, A. M., Chowdhury, F., Begum, Y. A., Khan, A. I., Faruque, A. S. G., Svennerholm, A.-M., Harris, J. B., Ryan, E. T., Cravioto, A., Calderwood, S. B., & Qadri, F. (2008). Shifting Prevalence of Major Diarrheal Pathogens in Patients

Seeking Hospital Care during Floods in 1998, 2004, and 2007 in Dhaka, Bangladesh. *The American Journal of Tropical Medicine and Hygiene*, 79(5), 708–714.

- Harris, J. B. (2018). Cholera: Immunity and Prospects in Vaccine Development. *The Journal of Infectious Diseases*, 218(suppl\_3), S141–S146. <https://doi.org/10.1093/infdis/jiy414>
- Harris, J. B., LaRocque, R. C., Qadri, F., Ryan, E. T., & Calderwood, S. B. (2012). Cholera. *Lancet*, 379(9835), 2466–2476. [https://doi.org/10.1016/S0140-6736\(12\)60436-X](https://doi.org/10.1016/S0140-6736(12)60436-X)
- Harro, C., Louis Bourgeois, A., Sack, D., Walker, R., DeNearing, B., Brubaker, J., Maier, N., Fix, A., Dally, L., Chakraborty, S., Clements, J. D., Saunders, I., & Darsley, M. J. (2019). Live attenuated enterotoxigenic *Escherichia coli* (ETEC) vaccine with dmLT adjuvant protects human volunteers against virulent experimental ETEC challenge. *Vaccine*, 37(14), 1978–1986. <https://doi.org/10.1016/j.vaccine.2019.02.025>
- Hasan, N. A., Choi, S. Y., Eppinger, M., Clark, P. W., Chen, A., Alam, M., Haley, B. J., Taviani, E., Hine, E., Su, Q., Tallon, L. J., Prosper, J. B., Furth, K., Hoq, M. M., Li, H., Fraser-Liggett, C. M., Cravioto, A., Huq, A., Ravel, J., ... Colwell, R. R. (2012). Genomic diversity of 2010 Haitian cholera outbreak strains. *Proceedings of the National Academy of Sciences of the United States of America*, 109(29), E2010–E2017. <https://doi.org/10.1073/pnas.1207359109>
- Hosangadi, D., Smith, P. G., & Giersing, B. K. (2019). Considerations for using ETEC and Shigella disease burden estimates to guide vaccine development strategy. *Vaccine*, 37(50), 7372–7380. <https://doi.org/10.1016/j.vaccine.2017.09.083>
- Hossain, M., Islam, K., Kelly, M., Mayo Smith, L. M., Charles, R. C., Weil, A. A., Bhuiyan, T. R., Kováč, P., Xu, P., Calderwood, S. B., Simon, J. K., Chen, W. H., Lock, M., Lyon, C. E., Kirkpatrick, B. D., Cohen, M., Levine, M. M., Gurwith, M., Leung, D. T., ... Ryan, E. T. (2019). Immune responses to O-specific polysaccharide (OSP) in North American adults infected with *Vibrio cholerae* O1 Inaba. *PLoS Neglected Tropical Diseases*, 13(11), e0007874. <https://doi.org/10.1371/journal.pntd.0007874>
- Hubbard, T. P., Billings, G., Dörr, T., Sit, B., Warr, A. R., Kuehl, C. J., Kim, M., Delgado, F., Mekalanos, J. J., Lewnard, J. A., & Waldor, M. K. (2018). A live vaccine rapidly protects against cholera in an infant rabbit model. *Science Translational Medicine*, 10(445), eaap8423. <https://doi.org/10.1126/scitranslmed.aap8423>



- Hullahalli, K., Pritchard, J. R., & Waldor, M. K. (2021). Refined Quantification of Infection Bottlenecks and Pathogen Dissemination with STAMPR. *MSystems*, 6(4), e0088721. <https://doi.org/10.1128/mSystems.00887-21>
- Isidean, S. D., Riddle, M. S., Savarino, S. J., & Porter, C. K. (2011). A systematic review of ETEC epidemiology focusing on colonization factor and toxin expression. *Vaccine*, 29(37), 6167–6178. <https://doi.org/10.1016/j.vaccine.2011.06.084>
- Jan, A. T. (2017). Outer Membrane Vesicles (OMVs) of Gram-negative Bacteria: A Perspective Update. *Frontiers in Microbiology*, 8. <https://www.frontiersin.org/articles/10.3389/fmicb.2017.01053>
- Kanungo, S., Azman, A. S., Ramamurthy, T., Deen, J., & Dutta, S. (2022). Cholera. *The Lancet*, 399(10333), 1429–1440. [https://doi.org/10.1016/S0140-6736\(22\)00330-0](https://doi.org/10.1016/S0140-6736(22)00330-0)
- Karlsson, S. L., Thomson, N., Mutreja, A., Connor, T., Sur, D., Ali, M., Clemens, J., Dougan, G., Holmgren, J., & Lebens, M. (2016). Retrospective Analysis of Serotype Switching of *Vibrio cholerae* O1 in a Cholera Endemic Region Shows It Is a Non-random Process. *PLoS Neglected Tropical Diseases*, 10(10), e0005044. <https://doi.org/10.1371/journal.pntd.0005044>
- Kennedy, E. A., King, K. Y., & Baldrige, M. T. (2018). Mouse Microbiota Models: Comparing Germ-Free Mice and Antibiotics Treatment as Tools for Modifying Gut Bacteria. *Frontiers in Physiology*, 9. <https://www.frontiersin.org/articles/10.3389/fphys.2018.01534>
- Khalil, I. A., Troeger, C., Blacker, B. F., Rao, P. C., Brown, A., Atherly, D. E., Brewer, T. G., Engmann, C. M., Houpt, E. R., Kang, G., Kotloff, K. L., Levine, M. M., Luby, S. P., MacLennan, C. A., Pan, W. K., Pavlinac, P. B., Platts-Mills, J. A., Qadri, F., Riddle, M. S., ... Reiner, R. C. (2018). Morbidity and mortality due to shigella and enterotoxigenic *Escherichia coli* diarrhoea: The Global Burden of Disease Study 1990–2016. *The Lancet. Infectious Diseases*, 18(11), 1229–1240. [https://doi.org/10.1016/S1473-3099\(18\)30475-4](https://doi.org/10.1016/S1473-3099(18)30475-4)
- Laviad-Shitrit, S., Izhaki, I., & Halpern, M. (2019). Accumulating evidence suggests that some waterbird species are potential vectors of *Vibrio cholerae*. *PLoS Pathogens*, 15(8), e1007814. <https://doi.org/10.1371/journal.ppat.1007814>
- Leitner, D. R., Lichtenegger, S., Temel, P., Zingl, F. G., Ratzberger, D., Roier, S., Schild-Prüfert, K., Feichter, S., Reidl, J., & Schild, S. (2015). A combined vaccine approach against *Vibrio cholerae* and ETEC based on outer membrane vesicles. *Frontiers in Microbiology*, 6, 823. <https://doi.org/10.3389/fmicb.2015.00823>

- Leung, D. T., Chowdhury, F., Calderwood, S. B., Qadri, F., & Ryan, E. T. (2012). Immune responses to cholera in children. *Expert Review of Anti-Infective Therapy*, 10(4), 435–444. <https://doi.org/10.1586/eri.12.23>
- Lieberman, L. A. (2022). Outer membrane vesicles: A bacterial-derived vaccination system. *Frontiers in Microbiology*, 13. <https://www.frontiersin.org/articles/10.3389/fmicb.2022.1029146>
- Linton, K. J., & Higgins, C. F. (1998). The Escherichia coli ATP-binding cassette (ABC) proteins. *Molecular Microbiology*, 28(1), 5–13. <https://doi.org/10.1046/j.1365-2958.1998.00764.x>
- Long, X., Ye, Y., Zhang, L., Liu, P., Yu, W., Wei, F., Ren, X., & Yu, J. (2016). IL-8, a novel messenger to cross-link inflammation and tumor EMT via autocrine and paracrine pathways (Review). *International Journal of Oncology*, 48(1), 5–12. <https://doi.org/10.3892/ijo.2015.3234>
- Longini, I. M., Nizam, A., Ali, M., Yunus, M., Shenvi, N., & Clemens, J. D. (2007). Controlling Endemic Cholera with Oral Vaccines. *PLoS Medicine*, 4(11), e336. <https://doi.org/10.1371/journal.pmed.0040336>
- Lopez, A. L., Deen, J., Azman, A. S., Luquero, F. J., Kanungo, S., Dutta, S., von Seidlein, L., & Sack, D. A. (2018). Immunogenicity and Protection From a Single Dose of Internationally Available Killed Oral Cholera Vaccine: A Systematic Review and Metaanalysis. *Clinical Infectious Diseases: An Official Publication of the Infectious Diseases Society of America*, 66(12), 1960–1971. <https://doi.org/10.1093/cid/cix1039>
- Lopez, A. L., Gonzales, M. L. A., Aldaba, J. G., & Nair, G. B. (2014). Killed oral cholera vaccines: History, development and implementation challenges. *Therapeutic Advances in Vaccines*, 2(5), 123–136. <https://doi.org/10.1177/2051013614537819>
- Lutz, C., Erken, M., Noorian, P., Sun, S., & McDougald, D. (2013). Environmental reservoirs and mechanisms of persistence of *Vibrio cholerae*. *Frontiers in Microbiology*, 4, 375. <https://doi.org/10.3389/fmicb.2013.00375>
- Malinverni, J. C., & Silhavy, T. J. (2009). An ABC transport system that maintains lipid asymmetry in the gram-negative outer membrane. *Proceedings of the National Academy of Sciences of the United States of America*, 106(19), 8009–8014. <https://doi.org/10.1073/pnas.0903229106>
- Mudrak, B., & Kuehn, M. J. (2010). Heat-Labile Enterotoxin: Beyond G M1 Binding. *Toxins*, 2(6), Article 6. <https://doi.org/10.3390/toxins2061445>

- Nelson, E. J., Harris, J. B., Morris, J. G., Calderwood, S. B., & Camilli, A. (2009). Cholera transmission: The host, pathogen and bacteriophage dynamic. *Nature Reviews. Microbiology*, 7(10), 10.1038/nrmicro2204. <https://doi.org/10.1038/nrmicro2204>
- Nelson, E. J., Nelson, D. S., Salam, M. A., & Sack, D. A. (2011). Antibiotics for Both Moderate and Severe Cholera. *New England Journal of Medicine*, 364(1), 5–7. <https://doi.org/10.1056/NEJMp1013771>
- New cholera cases in Africa surging fast, reach a third of 2022 total in a month.* (2023, March 1). WHO | Regional Office for Africa. <https://www.afro.who.int/news/new-cholera-cases-africa-surg-ing-fast-reach-third-2022-total-month>
- Nhu, N. T. Q., Lee, J. S., Wang, H. J., & Dufour, Y. S. (2021). Alkaline pH Increases Swimming Speed and Facilitates Mucus Penetration for *Vibrio cholerae*. *Journal of Bacteriology*, 203(7), e00607-20. <https://doi.org/10.1128/JB.00607-20>
- Nuzhat, S., Hossain, M. I., Shaly, N. J., Islam, R., Khan, S. H., Faruque, A. S. G., Bardhan, P. K., Khan, A. I., Chisti, M. J., & Ahmed, T. (2022). Different Features of Cholera in Malnourished and Non-Malnourished Children: Analysis of 20 Years of Surveillance Data from a Large Diarrheal Disease Hospital in Urban Bangladesh. *Children*, 9(2), 137. <https://doi.org/10.3390/children9020137>
- Ocasio, D. V. (2023). Cholera Outbreak—Haiti, September 2022–January 2023. *MMWR. Morbidity and Mortality Weekly Report*, 72. <https://doi.org/10.15585/mmwr.mm7202a1>
- Petousis-Harris, H. (2018). Impact of meningococcal group B OMV vaccines, beyond their brief. *Human Vaccines & Immunotherapeutics*, 14(5), 1058–1063. <https://doi.org/10.1080/21645515.2017.1381810>
- Qadri, F., Khan, A. I., Faruque, A. S. G., Begum, Y. A., Chowdhury, F., Nair, G. B., Salam, M. A., Sack, D. A., & Svennerholm, A.-M. (2005). Enterotoxigenic *Escherichia coli* and *Vibrio cholerae* Diarrhea, Bangladesh, 2004. *Emerging Infectious Diseases*, 11(7), 1104–1107. <https://doi.org/10.3201/eid1107.041266>
- Qadri, F., Svennerholm, A.-M., Faruque, A. S. G., & Sack, R. B. (2005). Enterotoxigenic *Escherichia coli* in Developing Countries: Epidemiology, Microbiology, Clinical Features, Treatment, and Prevention. *Clinical Microbiology Reviews*, 18(3), 465–483. <https://doi.org/10.1128/CMR.18.3.465-483.2005>
- Ramamurthy, T., Nandy, R. K., Mukhopadhyay, A. K., Dutta, S., Mutreja, A., Okamoto, K., Miyoshi, S.-I., Nair, G. B., & Ghosh, A. (2020). Virulence Regulation and Innate Host Response in the Pathogenicity of *Vibrio cholerae*. *Frontiers in*

*Cellular and Infection Microbiology*, 10.

<https://www.frontiersin.org/articles/10.3389/fcimb.2020.572096>

- Reeves, P. R., Hobbs, M., Valvano, M. A., Skurnik, M., Whitfield, C., Coplin, D., Kido, N., Klena, J., Maskell, D., Raetz, C. R. H., & Rick, P. D. (1996). Bacterial polysaccharide synthesis and gene nomenclature. *Trends in Microbiology*, 4(12), 495–503. [https://doi.org/10.1016/S0966-842X\(97\)82912-5](https://doi.org/10.1016/S0966-842X(97)82912-5)
- Research, C. for B. E. and. (2022). CBER-Regulated Products: Current Shortages. *FDA*. <https://www.fda.gov/vaccines-blood-biologics/safety-availability-biologics/cber-regulated-products-current-shortages>
- Rieckmann, A., Tamason, C. C., Gurley, E. S., Rod, N. H., & Jensen, P. K. M. (2018). Exploring Droughts and Floods and Their Association with Cholera Outbreaks in Sub-Saharan Africa: A Register-Based Ecological Study from 1990 to 2010. *The American Journal of Tropical Medicine and Hygiene*, 98(5), 1269–1274. <https://doi.org/10.4269/ajtmh.17-0778>
- Rodríguez, L., Cervantes, E., & Ortiz, R. (2011). Malnutrition and Gastrointestinal and Respiratory Infections in Children: A Public Health Problem. *International Journal of Environmental Research and Public Health*, 8(4), 1174–1205. <https://doi.org/10.3390/ijerph8041174>
- Roier, S., Zingl, F. G., Cakar, F., Durakovic, S., Kohl, P., Eichmann, T. O., Klug, L., Gadermaier, B., Weinzerl, K., Prassl, R., Lass, A., Daum, G., Reidl, J., Feldman, M. F., & Schild, S. (2016). A novel mechanism for the biogenesis of outer membrane vesicles in Gram-negative bacteria. *Nature Communications*, 7, 10515. <https://doi.org/10.1038/ncomms10515>
- Roier, S., Zingl, F. G., Cakar, F., & Schild, S. (n.d.). Bacterial outer membrane vesicle biogenesis: A new mechanism and its implications. *Microbial Cell*, 3(6), 257–259. <https://doi.org/10.15698/mic2016.06.508>
- Rolhion, N., & Chassaing, B. (2016). When pathogenic bacteria meet the intestinal microbiota. *Philosophical Transactions of the Royal Society B: Biological Sciences*, 371(1707), 20150504. <https://doi.org/10.1098/rstb.2015.0504>
- Roy, S. K., Buis, M., Weersma, R., Khatun, W., Chowdhury, S., Begum, A., Sarker, D., Thakur, S. K., & Khanam, M. (2011). Risk Factors of Mortality in Severely-malnourished Children Hospitalized with Diarrhoea. *Journal of Health, Population, and Nutrition*, 29(3), 229–235.
- Rytter, M. J. H., Kolte, L., Briend, A., Friis, H., & Christensen, V. B. (2014). The Immune System in Children with Malnutrition—A Systematic Review. *PLoS ONE*, 9(8). <https://doi.org/10.1371/journal.pone.0105017>

- Saluja, T., Mogasale, V. V., Excler, J.-L., Kim, J. H., & Mogasale, V. (2019). An overview of Vaxchora™, a live attenuated oral cholera vaccine. *Human Vaccines & Immunotherapeutics*, 16(1), 42–50. <https://doi.org/10.1080/21645515.2019.1644882>
- Scallan, E., Hoekstra, R. M., Angulo, F. J., Tauxe, R. V., Widdowson, M.-A., Roy, S. L., Jones, J. L., & Griffin, P. M. (2011). Foodborne Illness Acquired in the United States—Major Pathogens. *Emerging Infectious Diseases*, 17(1), 7–15. <https://doi.org/10.3201/eid1701.P11101>
- Schwechheimer, C., & Kuehn, M. J. (2015). Outer-membrane vesicles from Gram-negative bacteria: Biogenesis and functions. *Nature Reviews Microbiology*, 13(10), Article 10. <https://doi.org/10.1038/nrmicro3525>
- Sharma, P., Haycocks, J. R. J., Middlemiss, A. D., Kettles, R. A., Sellars, L. E., Ricci, V., Piddock, L. J. V., & Grainger, D. C. (2017). The multiple antibiotic resistance operon of enteric bacteria controls DNA repair and outer membrane integrity. *Nature Communications*, 8(1), Article 1. <https://doi.org/10.1038/s41467-017-01405-7>
- Shortage of cholera vaccines leads to temporary suspension of two-dose strategy, as cases rise worldwide.* (n.d.). Retrieved March 3, 2023, from <https://www.who.int/news/item/19-10-2022-shortage-of-cholera-vaccines-leads-to-temporary-suspension-of-two-dose-strategy--as-cases-rise-worldwide>
- Sit, B., Fakoya, B., & Waldor, M. K. (2022). Emerging Concepts in Cholera Vaccine Design. *Annual Review of Microbiology*, 76(1), 681–702. <https://doi.org/10.1146/annurev-micro-041320-033201>
- Sit, B., Fakoya, B., Zhang, T., Billings, G., & Waldor, M. K. (2021). Dissecting serotype-specific contributions to live oral cholera vaccine efficacy. *Proceedings of the National Academy of Sciences of the United States of America*, 118(7), e2018032118. <https://doi.org/10.1073/pnas.2018032118>
- Sit, B., Zhang, T., Fakoya, B., Akter, A., Biswas, R., Ryan, E. T., & Waldor, M. K. (2019). Oral immunization with a probiotic cholera vaccine induces broad protective immunity against *Vibrio cholerae* colonization and disease in mice. *PLoS Neglected Tropical Diseases*, 13(5), e0007417. <https://doi.org/10.1371/journal.pntd.0007417>
- Song, K. R., Lim, J. K., Park, S. E., Saluja, T., Cho, S.-I., Wartel, T. A., & Lynch, J. (2021). Oral Cholera Vaccine Efficacy and Effectiveness. *Vaccines*, 9(12), 1482. <https://doi.org/10.3390/vaccines9121482>

- Tan, K., Li, R., Huang, X., & Liu, Q. (2018). Outer Membrane Vesicles: Current Status and Future Direction of These Novel Vaccine Adjuvants. *Frontiers in Microbiology*, 9, 783. <https://doi.org/10.3389/fmicb.2018.00783>
- van Loon, F. P. L., Clemens, J. D., Chakraborty, J., Rao, M. R., Kay, B. A., Sack, D. A., Yunus, Md., Ali, Md., Svennerholm, A.-M., & Holmgren, J. (1996). Field trial of inactivated oral cholera vaccines in Bangladesh: Results from 5 years of follow-up. *Vaccine*, 14(2), 162–166. [https://doi.org/10.1016/0264-410X\(95\)00122-H](https://doi.org/10.1016/0264-410X(95)00122-H)
- Vibrio cholerae*-Induced Inflammation in the Neonatal Mouse Cholera Model | *Infection and Immunity*. (n.d.). Retrieved March 7, 2023, from <https://journals.asm.org/doi/10.1128/IAI.00054-14>
- Vidal, R. M., Muhsen, K., Tennant, S. M., Svennerholm, A.-M., Sow, S. O., Sur, D., Zaidi, A. K. M., Faruque, A. S. G., Saha, D., Adegbola, R., Hossain, M. J., Alonso, P. L., Breiman, R. F., Bassat, Q., Tamboura, B., Sanogo, D., Onwuchekwa, U., Manna, B., Ramamurthy, T., Levine, M. M. (2019). Colonization factors among enterotoxigenic *Escherichia coli* isolates from children with moderate-to-severe diarrhea and from matched controls in the Global Enteric Multicenter Study (GEMS). *PLoS Neglected Tropical Diseases*, 13(1), e0007037. <https://doi.org/10.1371/journal.pntd.0007037>
- Waldor, M. K., & Mekalanos, J. J. (1996). Lysogenic conversion by a filamentous phage encoding cholera toxin. *Science (New York, N.Y.)*, 272(5270), 1910–1914. <https://doi.org/10.1126/science.272.5270.1910>
- Wolf, M. K. (1997). Occurrence, distribution, and associations of O and H serogroups, colonization factor antigens, and toxins of enterotoxigenic *Escherichia coli*. *Clinical Microbiology Reviews*, 10(4), 569–584.
- Zhang, Y., Tan, P., Zhao, Y., & Ma, X. (n.d.). Enterotoxigenic *Escherichia coli*: Intestinal pathogenesis mechanisms and colonization resistance by gut microbiota. *Gut Microbes*, 14(1), 2055943. <https://doi.org/10.1080/19490976.2022.2055943>
- Zilberberg, A., Ofek, I., & Goldhar, J. (1984). Affinity of adherence in vitro and colonization of mice intestine by enterotoxigenic *Escherichia coli* (ETEC). *FEMS Microbiology Letters*, 23(1), 103–106. <https://doi.org/10.1111/j.1574-6968.1984.tb01043.x>
- Zingl, F. G., Kohl, P., Cakar, F., Leitner, D. R., Mitterer, F., Bonnington, K. E., Rechberger, G. N., Kuehn, M. J., Guan, Z., Reidl, J., & Schild, S. (2020). Outer Membrane Vesiculation Facilitates Surface Exchange and In Vivo Adaptation of *Vibrio cholerae*. *Cell Host & Microbe*, 27(2), 225-237.e8. <https://doi.org/10.1016/j.chom.2019.12.002>

**CURRICULUM VITAE**

